

Journal of Visualized Experiments

A guide to structured illumination TIRF microscopy at high speed with multiple colors --Manuscript Draft--

Manuscript Number:	JoVE53988R4
Full Title:	A guide to structured illumination TIRF microscopy at high speed with multiple colors
Article Type:	Invited Methods Article - JoVE Produced Video
Keywords:	Optical superresolution; structured illumination microscopy; Fluorescence; high speed imaging; TIRF; bioimaging
Manuscript Classifications:	5.5.595.458: Microscopy, Fluorescence; 5.5.595.690: Microscopy, Video; 8.1.671.617.562: Microscopy
Corresponding Author:	Florian Ströhl University of Cambridge Cambridge, Cambridgeshire UNITED KINGDOM
Corresponding Author Secondary Information:	
Corresponding Author E-Mail:	fs417@cam.ac.uk
Corresponding Author's Institution:	University of Cambridge
Corresponding Author's Secondary Institution:	
First Author:	Laurence J Young
First Author Secondary Information:	
Other Authors:	Laurence J Young Clemens F Kaminski
Order of Authors Secondary Information:	
Abstract:	Optical super-resolution imaging with structured illumination microscopy (SIM) is a key technology for the visualization of processes at the molecular level in the chemical and biomedical sciences. Although commercial SIM systems are available, systems that are custom designed in the laboratory can outperform commercial systems, the latter typically designed for ease of use and general purpose applications, both in terms of imaging fidelity and speed. This article presents an in-depth guide to building a SIM system that uses total internal reflection (TIR) illumination and is capable of imaging at up to 10 Hz in three colors at a resolution reaching 100 nm. Due to the combination of SIM and TIRF, the system provides better image contrast than rival technologies. To achieve these specifications, several optical elements are used to enable automated control over the polarization state and spatial structure of the illumination light for all available excitation wavelengths. Full details on hardware implementation and control are given to achieve synchronization between excitation light pattern generation, wavelength, polarization state, and camera control with an emphasis on achieving maximum acquisition frame rate. A step-by-step protocol for system alignment and calibration is presented and the achievable resolution improvement is validated on ideal test samples. The capability for video-rate super-resolution imaging is demonstrated with living cells.
Author Comments:	
Additional Information:	
Question	Response
If this article needs to be filmed by a certain date to due to author/equipment/lab availability, please indicate the date below and explain in your cover letter.	

If this article needs to be "in-press" by a certain date to satisfy grant requirements, please indicate the date below and explain in your cover letter.

TITLE:

A guide to structured illumination TIRF microscopy at high speed with multiple colors

AUTHORS:

Young, Laurence J
Department of Chemical Engineering and Biotechnology
University of Cambridge
Cambridge, United Kingdom
ljy24@cam.ac.uk

Ströhl, Florian
Department of Chemical Engineering and Biotechnology
University of Cambridge
Cambridge, United Kingdom
fs417@cam.ac.uk

Kaminski, Clemens F
Department of Chemical Engineering and Biotechnology
University of Cambridge
Cambridge, United Kingdom
cfk23@cam.ac.uk

CORRESPONDING AUTHOR:

Young, Laurence J

KEYWORDS:

Optical super-resolution, structured illumination microscopy, fluorescence, high speed imaging, TIRF, bioimaging

SHORT ABSTRACT:

This article provides an in depth guide for the assembly and operation of a structured illumination microscope operating with total internal reflection fluorescence illumination (TIRF-SIM) to image dynamic biological processes with optical super-resolution in multiple colors.

LONG ABSTRACT:

Optical super-resolution imaging with structured illumination microscopy (SIM) is a key technology for the visualization of processes at the molecular level in the chemical and biomedical sciences. Although commercial SIM systems are available, systems that are custom designed in the laboratory can outperform commercial systems, the latter typically designed for ease of use and general purpose applications, both in terms of imaging fidelity and speed. This article presents an in-depth guide to building a SIM system that uses total internal reflection (TIR) illumination and is capable of imaging at up to 10 Hz in three colors at a resolution reaching 100 nm. Due to the combination of SIM and TIRF, the system provides better image contrast than rival technologies. To achieve these specifications, several optical elements are used to enable automated control over the polarization state and spatial structure of the illumination light for all available excitation wavelengths. Full details on hardware implementation and control are given to achieve synchronization between excitation light pattern generation, wavelength, polarization state, and camera control with an emphasis on achieving maximum acquisition frame rate. A step-by-step protocol for system

alignment and calibration is presented and the achievable resolution improvement is validated on ideal test samples. The capability for video-rate super-resolution imaging is demonstrated with living cells.

INTRODUCTION:

Over the last half a decade, super-resolution microscopy has matured and moved from specialist optics labs into the hands of the biologist. Commercial microscope solutions exist for the three main variants for achieving optical super-resolution: single molecule localization microscopy (SMLM), stimulated emission depletion microscopy (STED), and structured illumination microscopy (SIM)^{1,2}. SMLM such as photoactivated localization microscopy (PALM) and stochastic optical reconstruction microscopy (STORM) have been the most popular techniques, largely due to the simplicity of the optical setup and the promise of high spatial resolution, readily down to 20 nm. However super-resolution microscopy *via* single molecule localization comes with an intrinsic trade-off: the spatial resolution attainable is dependent on accumulating a sufficient number of individual fluorophore localizations, hence limiting the temporal resolution. Imaging dynamic processes in live cells therefore becomes problematic as one must adequately sample the movement of the structure of interest to prevent motion artifacts while also acquiring enough localization events in that time to reconstruct an image. In order to meet these requirements, live cell SMLM demonstrations have obtained the required increase in fluorophore photoswitching rates by greatly increasing the excitation power, and this leads in turn to phototoxicity and oxidative stress, thereby limiting sample survival times and biological relevance³.

A clear advantage of STED over both SIM and SMLM is that it can image with super-resolution in thick samples, for example lateral resolution of around 60 nm was achieved in organotypic brain slices at depths up to 120 μm ⁴. Imaging at such depths with single objective implementations of SMLM or SIM is unfeasible, but becomes possible with either single-molecule light sheet or lattice light sheet microscopy⁵. Video-rate STED has also been demonstrated and used to map synaptic vesicle mobility, although so far this has been limited to imaging small fields of view⁶.

For applications in cell biology and molecular self-assembly reactions^{7–12} that require imaging with high temporal resolution over many time points, structured illumination microscopy (SIM) can be well-suited as it is not dependent on the photophysical properties of a particular fluorescent probe. Despite this inherent advantage of SIM, up to now its use has been mainly confined to imaging fixed cells or slow moving processes. This is due to the limitations of commercially available SIM systems: the acquisition frame rate of these instruments was limited by the rotation speed of the gratings used to generate the required sinusoidal illumination patterns as well as the polarization maintaining optics. The newest generation of commercial SIM instruments are capable of fast imaging but they are prohibitively expensive to all but central imaging facilities.

This protocol presents a guide to the construction of a flexible SIM system for imaging fast processes in thin samples and near the basal surface of living cells. It employs total internal reflection fluorescence (TIRF) to generate an illumination pattern which penetrates no deeper than approximately 150 nm into the sample¹³ which vastly reduces the out of focus background signal. The idea of combining SIM with TIRF is almost as old as SIM itself¹⁴ but was not realized experimentally before 2006¹⁵. The first *in vivo* images obtained with TIRF-SIM were reported in 2009¹⁶ achieving frame rates of 11 Hz to visualize tubulin and kinesin dynamics, and two color TIRF-SIM systems have been presented^{17,18}. Most recently, a guide

for the construction and use of a single color two-beam SIM system was presented featuring frame-rates of up to 18 Hz^{19,20}.

The set-up presented here is capable of SIM super-resolution imaging at 20 Hz in three colors, two of which can be operated in TIRF-SIM. The whole system is constructed around an inverted microscope frame and uses a motorized xy translation stage with a piezo-actuated z stage. To generate the sinusoidal excitation patterns required for TIRF-SIM, the system presented uses a ferroelectric spatial light modulator (SLM). Binary grating patterns are displayed on the SLM and the resulting ± 1 diffraction orders are filtered, relayed and focused into the TIR ring of the objective lens. The necessary phase shifts and rotations of the gratings are applied by changing the displayed SLM image. This protocol describes how to build and align such an excitation path, details the alignment of the emission path, and presents test samples for ensuring optimal alignment. It also describes the issues and challenges particular to high speed TIRF-SIM regarding polarization control and synchronization of components.

Design Considerations and Constraints

Before assembling the TIRF-SIM system presented in this protocol, there are several design constraints to consider which determine the choice of optical components. All abbreviations of optical components refer to Figure 1.

Spatial Light Modulator (SLM)

A binary ferroelectric SLM is used in this setup as it is capable of sub-millisecond pattern switching. Grayscale nematic SLMs may be used but these offer greatly reduced switching times. Each on or off pixel in a binary phase SLM will impart either a π or 0 phase offset to the incident plane wavefront, therefore if a periodic grating pattern is displayed on the SLM it will operate as a phase diffraction grating.

Total internal reflection (TIR)

To achieve TIR and produce an evanescent field, the incident angle of the excitation beams at the glass-sample interface must be greater than the critical angle θ_c . This sets the minimum incident angle required, and hence also the maximum spacing, or period, of the evanescent illumination pattern. The maximum incident angle θ_{max} (the acceptance angle) is limited by the numerical aperture (NA) of the objective lens which can be calculated from the definition $NA = n \sin(\theta_{max})$. This determines the minimum pattern spacing achievable according to the Abbe formula $\Delta x = \frac{\lambda}{2NA}$ which links NA and wavelength λ to the minimum pattern spacing Δx . In practice, a 1.49 NA oil immersion TIRF objective yields a maximum angle of incidence of around 79° and a minimum pattern period on the sample of 164 nm using an excitation wavelength of 488 nm. These two angles define a ring in the back aperture of the objective over which the instrument achieves TIR illumination (i.e. the TIR ring) and in which the two excitation foci must be accurately positioned and precisely rotated to generate each illumination pattern.

Reconstruction of TIRF-SIM images requires the acquisition of a minimum of three phase shifts per pattern rotation therefore the SLM pattern period must be divisible by 3 (see Fig 1). For example, a period of 9 pixels for 488 nm illumination and 12 pixels for 640 nm illumination. For a comprehensive discussion of SLM pattern design, including sub-pixel optimization of pattern spacing using sheared gratings, see the previous work of Kner et al¹⁶ and Lu-Walther et al²⁰. The position of the two excitation foci must be inside the TIR ring for

all wavelengths, however the diffraction angle of the ± 1 orders from the SLM is wavelength dependent. For standard SIM, multicolor imaging can be achieved by optimizing the grating period for the longest wavelength, and tolerating a loss in performance for the shorter channels. For TIRF-SIM however, optimizing for one wavelength means that the other wavelength foci are no longer within the TIR ring. For example, using a grating period of 9 pixels is sufficient to provide TIRF for 488 nm, as the foci are at 95% of the diameter of the back aperture and within the TIR ring, but for 640 nm this period would position the foci outside the aperture. For this reason different pixel pattern spacings must be used for each excitation wavelength.

The alignment of the TIRF-SIM excitation path is extremely sensitive to small changes in the position of the dichroic mirror (DM4 in Fig 1) in the microscope body, much more so than in conventional SIM. Use of a rotating filter cube turret is not recommended, instead use a single, multi-band dichroic mirror, which is kept in a fixed position and designed specifically for the excitation wavelengths used. It is essential that only the highest quality dichroic mirrors are used. These require thick substrates of at least 3 mm, and are often designated as “imaging flat” by manufacturers. All other substrates lead to intolerable aberration and image degradation in TIRF-SIM.

Polarization control

To achieve TIRF-SIM it is essential to rotate the polarization state of the excitation light in synchronicity with the illumination pattern such that it remains azimuthally polarized in the objective pupil plane with respect to the optical axis (i.e. s-polarized). Alignment of the polarization control optics will depend on the specific optical element employed, for example a Pockels cell²¹, or a half wave plate in a motorized rotation stage²². In this protocol a custom liquid crystal variable retarder (LCVR) is used, designed to provide full-wave (2π) retardance over the wavelength range 488 to 640 nm as it allows fast (\sim ms) switching. If using a liquid crystal retarder it is essential to use a high quality component: standard components are typically not stable enough to give a constant retardance over the length of the camera exposure time which leads to a blurring out of the illumination pattern and low modulation contrast. Liquid crystal retarders are also strongly temperature dependent and require built in temperature control.

Synchronization

The lasers must be synchronized with the SLM. Binary ferroelectric SLMs are internally balanced by switching between an on state and off state. The pixels only act as half wave plates in either their on or off state, but not during the interframe switching time. Therefore the lasers should only be switched on during on/off states via the LED Enable signal from the SLM to prevent a reduction in pattern contrast due to the intermediate state of the pixels. An acousto-optic modulator (AOM) could alternatively be used as a fast shutter if the lasers cannot be digitally modulated.

Choice of lenses

Based on these constraints, the required demagnification of the SLM plane onto the sample plane to produce the desired illumination patterns can be determined. This allows calculation of the focal lengths of the two lenses L3 and L4 in the image relay telescope and the excitation tube lens L5. In this system a 100X/1.49NA oil immersion objective lens is used with 488 nm and 640 nm excitation, hence uses focal lengths of 300 and 140 mm for L4 and L3, and 300 mm for L5, giving a total demagnification of 357x, equivalent to an SLM pixel size of 38 nm at the sample plane. Using this combination of lenses, SLM grating periods of

9 for 488 nm illumination and 12 pixels for 640 nm give pattern spacings of 172 and 229 nm at the sample, corresponding to angles of incidence of 70° and 67° respectively. For a glass-water interface, the critical angle is 61°, and is independent of wavelength, therefore these two pattern spacings allow TIRF excitation for both wavelengths. An objective lens equipped with a correction collar is useful for correction of spherical aberrations introduced by variations in coverslip thickness, or if operating at 37°C.

Image Reconstruction

Once raw SIM data has been acquired it is a matter of computational effort to generate super-resolved images in a two-step process. Firstly, the illumination pattern has to be determined for every image and secondly, the components of the SIM spectrum must be separated and recombined appropriately as to double the effective OTF support (see Figure 6 insets).

Precise knowledge of the projected illumination patterns is paramount, as the super-resolved frequency components have to be unmixed as accurately as possible to prevent artifacts caused by the residual parts of overlapping components. We determine the illumination pattern parameters *a posteriori* from the raw image data following the procedure introduced by Gustafsson et al.²³. In short, a set of illumination parameters that describes a normalized two-dimensional sinusoid has to be found for each of the m excitation patterns $e^{om}(x, y)$:

$$e^{om}(x, y) = \frac{1}{2} + \frac{c_m}{2} \cos(k_{ox}x + k_{oy}y + \varphi_m).$$

Hereby c_m and φ_m describe the fringe contrast and the pattern starting phase of each individual image m respectively. The components of the wave vector, k_{ox} and k_{oy} , only change with different orientations o of the pattern and can be assumed to be otherwise constant. To coarsely determine the components of the wave vector a cross correlation of raw image spectra is performed, which is refined by applying subpixel shifts to one of the cross-correlated images as to optimize the overlap. This is done via multiplication of real-space phase gradients $\Delta = e^{-i(\delta_x x + \delta_y y)}$ that induce a subpixel shift in frequency-space. Note that it is useful to have a good estimate of the wave-vectors prior to the actual pattern estimation and this can be found by imaging a fluorescent bead layer.

As the phase step between shifted patterns is $2\pi/3$, i.e. $\varphi_m = \varphi_0 + m \frac{2\pi}{3}$, the separation of frequency components can be performed by a Fourier transform along the “phase axis”. The global phase φ_0 and the fringe contrast c_m can then be determined using complex linear regression of different components. The individual separated components are then combined using a generalised Wiener filter. For a detailed description of both parameter extraction and implementation of the generalized Wiener filter we refer the reader to Gustafsson et al.²³ where the same algorithm is used.

PROTOCOL:

1. Arranging and aligning the excitation path

1.1. **Mark the positions of the components on the optical table (see Figure 1 for an overview of the optical setup).** Separate the objective, lenses L3, L4, L5, and the SLM each by the sum of their respective focal lengths such that the SLM surface will be relayed onto the focal plane of the objective.

1.2. Insert multi-edge dichroic mirror DM4 into the filter cube turret of the microscope frame.

1.3. Insert the second dichroic mirror DM3 into a 1" square kinetic mirror mount, and position it one focal length away from the tube lens L5.

Note: This excitation path design incorporates two identical dichroic mirrors DM3 and DM4 which are taken from the same production batch to ensure identical optical properties. The dichroic mirror (DM4) is positioned such that the s- and p- axes are switched compared to the dichroic located in the microscope (DM3) thereby cancelling any polarization ellipticity introduced by its birefringence (Figure 1). This compensation works equally well for each illumination wavelength. This step is essential for maintaining high modulation contrast.

1.4. Before inserting any lenses into the excitation path, accurately define the optical axis for the system.

1.4.1. Remove the objective lens (OB) from the turret and instead screw in an alignment tool. This consists of a 300 mm long optical cage system with two alignment disks at both ends.

1.4.2. Use the dichroic mirror DM3 and a temporary alignment mirror positioned at the approximate later location of the SLM to steer a collimated reference beam from Laser 1 through the center of the holes in the two alignment disks. Direct the beam from Laser 1 to the temporary mirror as depicted in Figure 1 using three mirrors and dichroic mirror DM2. The temporary mirror at the SLM position must be close to perpendicular to the optical axis.

Note: Use Laser 1 as the reference beam, as the other lasers can be subsequently aligned once the excitation path is in place.

1.4.3. Remove the alignment tool once the coarse optical axis has been determined. Insert an iris into the beam path before it enters the microscopy body and center it on the beam. Attach a piece of white card with a small hole centered on the iris. Reinsert the objective lens (OB).

Note: The beam leaving the objective will now be highly divergent, but there will be a very weak reflection from the back surface of the lens that will be visible on the white card. All lenses, even if they are anti-reflection coated, will have weak back reflections that can be used to ensure coaxial alignment. If the beam is exactly perpendicular to the lens then the back reflection will go back through the center of the iris.

1.4.4. Make iterative angular adjustments to the two mirrors (DM3 and alignment mirror at the SLM position) to center the back reflection on the card with the incoming beam. Temporarily remove the objective lens (OB) and mark the laser spot on the ceiling to create a reference position.

1.4.5. Insert a pair of irises at the height of the reference beam along the threaded holes of the table. The beam should be parallel to the surface of the optical table. The optical axis is now defined.

1.5. Insert the tube lens (L5) roughly one focal length away from the objective. Mount this lens on a linear translation stage set to translate along the direction of the reference beam.

1.6. Adjust the tube lens position and angle such that the beam leaving the objective is collimated and hits the reference spot on the ceiling. Check that the lens is perpendicular to the beam by again checking the back reflection with the iris and white card. Remove the objective lens (OB) and insert the second lens of the image relay telescope (L4).

Note: Ensuring proper collimation and non-deflection of the beam is made easier when there is an even number of lenses in the beam path.

1.7. Adjust the position and angle of this lens using a linear translation stage to maintain collimation and to ensure the reference beam still hits the marked spot on the ceiling.

1.8. Replace the objective lens (OB) and insert the first lens of the telescope (L3). Adjust the position and angle of this lens to ensure collimation and non-deflection, as described in previous steps.

1.9. Mount the SLM chip on a gimbal mount which provides rotation without translation about the center of the chip surface.

Note: The specific mounting design depends on the SLM used. If the SLM is supplied without a mount, it should be fixed to a custom machined aluminum plate which is then attached to a lens gimbal mount.

1.10. With the lenses aligned, insert the SLM in place of the mirror. Adjust the position of the SLM such that the reference beam is located at the center of the SLM chip, and adjust the angle such that the beam passes through the two relay lenses (L3 and L4). Check that the reference beam is still centered on the marked spot.

1.11. Expand and collimate the reference beam using a Keplerian beam expander.

1.11.1. Mount the two lenses (L1 and L2) in a cage system for ease of adjustment.

1.11.2. Centre the cage system on the reference beam by removing the lenses and replacing them with irises.

1.11.3. Insert the two lenses and adjust the axial position of L2 to collimate the expanded beam using a shearing interferometer. L2 should be one focal length away from the surface of the SLM.

1.11.4. Check that the expanded beam is still collimated after the two relay lenses L3 and L4. Use the shearing interferometer just after DM3 to check for collimation.

1.12. Once the excitation path has been aligned for a single wavelength, couple the other two lasers into the beam path. Steer each beam through two irises centered on the excitation path using the beam combining dichroic mirrors (DM1 and DM2).

2. Alignment of polarization rotator

2.1. Mount the LCVR with its fast axis at 45° to the incident polarization.

2.2. Fine tune polarization angle of the beam incident to the LCVR using an achromatic half wave plate (HWP) by inserting the HWP and the LCVR between crossed polarizers. Rotate the HWP to minimize the transmitted power.

Note: In order to act as a variable polarization rotator, the fast axis of the liquid crystal retarder (LCVR) must be precisely aligned at 45° to the incident vertical beam polarization. The LCVR is physically mounted at 45° but this is only a coarse alignment. The HWP is used to ensure perfect 45° alignment of the incident polarization with respect to the LCVR fast axis. The quarter wave plate (QWP) converts the tilted elliptical polarization induced by the LCVR back to linear polarization at an angle controlled by the applied voltage²⁴.

2.3. Insert the QWP after the LCVR and rotate it to align its slow axis to the incoming polarization by minimizing the transmitted power between crossed polarizers.

3. Alignment of the emission path

3.1. Coarsely position the camera using a stage micrometer slide and transmitted light.

3.1.1. Focus on the reticle using the microscope oculars and fix the objective lens at this position.

3.1.2. Roughly center the camera and move the camera position to bring the image of the reticle into focus by observing the image on screen.

Note: If an external filter wheel is used then the filter cube will not contain an emission filter, therefore the oculars must not be used when lasers are switched on.

3.2. Finely adjust the camera position using a fluorescent bead sample.

3.2.1. Prepare a monolayer of fluorescent beads by spreading a drop of 100 nm multicolor beads on a #1.5 coverglass. Leave to dry to adsorb the beads to the coverglass and then re-immerses in water.

3.2.2. Place the bead sample onto the objective with immersion oil. Finely adjust the position of the camera such that the fluorescent bead layer is in focus. Do not adjust the objective lens position once the focus has been found.

Note: As the SLM must be in a plane conjugate to the sample plane, the position of the SLM, relay lenses, and objective must be fixed. To adjust the focus, move the sample axially instead of the objective using a piezo z-stage.

3.3. Generate the appropriate SIM binary grating patterns as bitmap files.

3.3.1. For 2D/TIRF-SIM, generate a series of 9 binary grating images: 3 pattern orientations each with 3 equally spaced phase shifts. Generate these numerically (using MATLAB for example) from a rotated 2D sinusoid with a phase offset applied, then thresholding to produce a binary image. See Supplemental Code Files for example code.

3.3.2. For alignment purposes, also generate grating patterns that have been windowed by a small circular aperture for each of the 3 orientations, as shown in Figure 2. The windowed alignment gratings do not need to be externally triggered but can be manually switched by the user via the SLM's software.

Note: See references for a discussion of the optimal rotation angles and an example of grating pattern generation code^{16,20}.

3.4. Upload the bitmap images to the SLM using the manufacturer's software (for example MetroCon).

3.4.1. Load the SLM control software and click "Connect".

3.4.2. In the "Repertoire" tab, click "Load" to open the repertoire file and check the number of Running Orders contained in the file. In the example repertoire file given there are five Running Orders.

3.4.3. Click "Send to Board" to upload the repertoire file to the SLM.

3.4.4. Wait for the bitmap images to upload and for the device to automatically reboot.

Note: An example repertoire file, which contains grating bitmap images and a file defining the order, is included as a Supplemental Code File. The ".repz" file may be opened using ZIP file archiver software.

3.5. Display a windowed alignment grating on the SLM for the first orientation (for example 0°).

3.5.1. In the SLM control software, select the "Status" tab, enter the number of the Running Order (in the case of the example file, this is Running Order "1").

3.5.2. Click "Select" to change the Running Order to the alignment grating.

Note: This will illuminate a small circular region in the sample plane. If the SLM surface is correctly conjugated to the sample plane then the edges of this region will be sharply in focus. The grating pattern will produce multiple diffraction orders at the focus of L3: the zero order reflection from the reflective backplane of the SLM, the -1 and +1 orders corresponding to the grating, and also weaker higher orders that arise from diffraction of internal elements specific to the SLM device (e.g. reflections of the internal wirings of the SLM pixels and irregularities at the pixel edges). All but the -1 and +1 orders must be filtered out.

3.6. Insert a spatial mask (SM) mounted in an x,y stage into the beam path at the focal position of L3, and translate its position with respect to the optical axis such that only the desired first orders are passed. Directly after the spatial filter, only two circular beams will be visible.

Note: The spatial mask is fabricated by punching 6 holes into aluminum foil using a needle. The holes should be large enough to pass the first order beams for all laser wavelengths. A detailed analysis of the spatial mask is given in reference²⁰.

3.7. Display the next orientation of the alignment grating (60° , running order 2) and again ensure that only the first orders are let through the spatial mask, adjusting its position if required.

3.8. Repeat for the final orientation (120° , running order 3).

3.9. Check the image of the fluorescent bead layer on the camera. If the two circular beams are not overlapping as depicted in Figure 2 then reposition the sample plane by iteratively adjusting the objective lens and camera position.

3.10. Adjust the objective position to overlap the two beams which will bring the image out of focus. Reposition the camera to bring the image back into focus and fine tune the objective in case two circles are still visible. Repeat this process until the two beams overlap and a single circular region is in focus.

3.11. Once the position of the sample plane has been set, keep the objective position fixed.

3.12. To confirm TIRF illumination, image a solution of fluorescent dye, for example for a 488 nm excitation wavelength, use a solution of 10 μM rhodamine 6G.

3.12.1. Bring the dye sample into focus. If the two beams are incident at the correct TIRF angle then single molecules will be visible without high background, and the edges of the circular aperture will be in focus. See Figure 2B-D for examples of aligned and misaligned TIRF beams.

3.12.2. Display each orientation of the windowed gratings in turn and ensure that all three orientations provide TIRF illumination and that the two beams overlap at the sample plane. Fine adjustments to the position of the beams can be made by adjusting dichroic mirror DM3.

Note: Although different wavelengths are focused at slightly different positions due to axial chromatic aberration, this is not critical and may be corrected by applying a constant z-offset to the sample position prior to excitation with the second wavelength.

4. System synchronization and calibration

4.1. Place the bead monolayer sample on the objective and bring into focus.

4.2. Program the SLM using its control software to display each of the 3 phase shift images in turn, for the first pattern orientation (0°).

4.2.1. Using the SLM control software, switch to Running Order 4 of the example repertoire.

4.2.2. Configure the camera using its acquisition software (for example HCSImage) to output two signals: one positive and one negative TTL trigger signal during the global exposure period. In the camera software, under “Advanced Camera Properties”, set Output Trigger Kind 1 and 2 to “Exposure”, and Output Trigger Polarity 1 and 2 to “Positive” and “Negative” respectively.

4.2.3. Connect Output 1 and 2 of the camera to the “Trigger” and “Finish” inputs of the SLM respectively, using coaxial cables. The SLM is now synchronized to the camera.

4.3. Acquire a series of 3 images.

4.3.1. In the “Sequence” pane, select “Hard Disk Record” as the scan type, and set the frame count to 3.

4.3.2. Click “Start” to acquire 3 frames. The SLM pattern will change upon each exposure. The fluorescent beads in the image will appear to blink on and off between each of the 3 images. The amount of blinking is a read out of the modulation contrast of the sinusoidal illumination pattern.

4.4. Rotate the polarization of the excitation laser with the LCVR using custom software in order to achieve azimuthal polarization and therefore the highest modulation contrast for the given pattern orientation.

4.4.1. Load the LCVR calibration software.

4.4.2. Enter 0 and 8 for the Minimum and Maximum Voltage respectively.

4.4.3. Click “Sweep LCVR Voltage” to rotate the polarization.

Note: The LCVR retardance is a function of temperature and can drift day-to-day even with temperature control. In this step, optimal azimuthal polarization is found empirically by sweeping the applied voltage between its minimum and maximum voltage which has the effect of rotating the polarization incident at the sample. The modulation contrast is calculated for each voltage²⁵ and the voltage that achieves peak contrast is used in the following steps.

4.4.4. Wait for the calibration process to complete, and note down the measured voltage.

4.5. Repeat this calibration process for the remaining two pattern orientations (60° and 120°) and each of the excitation wavelengths.

4.6. Synchronize the camera exposure with the LCVR, lasers, emission filter wheel and piezo z-stage²⁶. To accomplish this, use a high speed data acquisition (DAQ) board as the master clock source for the system, and use the SLM’s LED Enable output signal to modulate the lasers (see Figure 3B).

Note: The specific implementation is dependent on the components used but the use of a high speed DAQ board for digital trigger synchronization and control of the LCVR using an analog voltage, controlled via software, is recommended. The control software used in this protocol is available upon request.

4.7. Due to axial chromatic aberration, for each wavelength, also apply a z-offset to the sample stage.

4.7.1. Determine the offset experimentally by focusing on a multicolor bead monolayer sample at the first wavelength (e.g. 488 nm) then switching to the second (e.g. 640 nm). The beads will now be out of focus.

4.7.2. Refocus the beads and measure the change in z position that was needed. This offset can then be applied to the piezo z-stage every time the excitation wavelength is changed.

4.8. Using the SLM control software, switch the SLM Running Order to the full series of 9 binary grating images required for TIRF-SIM. This is Running Order 0 in the example repertoire.

4.9. Using the camera control software, acquire 9 images of the bead sample.

4.9.1. In the “Sequence” pane of the camera software, select “Hard Disk Record” as the scan type, and change the frame count to 9.

4.9.2. Click “Start” to acquire images.

4.9.3. Save the acquired images as TIFF files by selecting “TIFF” as the image type in the “Save Buffered Images” window, and clicking OK.

4.10. Reconstruct a super-resolution image from the raw TIFF images using commercial or custom software to validate the improvement in resolution over standard TIRF.

Note: For our microscope we use custom reconstruction code developed both in-house and by Dr Lin Shao²⁷.

REPRESENTATIVE RESULTS:

Multicolor 100nm diameter fluorescent beads were imaged to compare standard TIRF to TIRF-SIM and quantify the attainable improvement in lateral resolution (Figure 4A-B). Reconstruction of raw frames into super-resolution images was performed using standard algorithms as outlined in the literature^{27,28}. It can be seen that TIRF-SIM clearly has significantly higher lateral resolution compared to TIRF. The point spread function (PSF) of a microscope is well approximated by the image of a single sub-diffraction sized fluorescent bead, therefore the PSF and the resolution can be quantified by fitting 2D Gaussian functions to individual beads for each wavelength. The estimated resolution of the microscope based on the mean value of the full width half maximum (FWHM) is 89 nm and 116 nm for 488 and 640 nm TIRF-SIM respectively (Figure 4C). This corresponds to a two-fold improvement in lateral resolution for both wavelengths compared to the theoretical diffraction limited case. Fluorescently labelled amyloid fibrils are also an excellent test sample for demonstrating doubled resolution (Figure 4D). Amyloid fibrils were formed *in vitro* by incubating β -amyloid labelled with 10% rhodamine derivative dyes (488 nm excitation) for 1 week and subsequently imaging with TIRF-SIM. See reference¹² for more information.

Subcellular structures with high contrast such as emGFP labelled microtubules (Figure 5B, G) or LifeAct-GFP (Figure D) are ideal for TIRF-SIM imaging and yield high contrast super-resolution images. TIRF-SIM imaging using the setup detailed in this protocol enables observation of a sub-population of microtubules located in the vicinity of the basal cell cortex, and microtubule polymerization and depolymerization can be seen over time (Animated Figure 1). Not all samples are amenable to imaging with TIRF-SIM, in particular, low contrast samples without discrete structures. Cells expressing cytosolic GFP lack high resolution information aside from at the edges of the plasma membrane (Figure 5 F, H and Animated Figure 2) and are hence sub-optimal for TIRF-SIM imaging as the resulting

reconstructions are essentially TIRF images overlaid with artifacts. In such samples, the increase in contrast can often be attributed to the deconvolution step of the reconstruction algorithm.

High modulation contrast is essential for successful SIM imaging. The Fourier transform of the reconstructed image allows visualization of the SIM optical transfer function (OTF) (Figure 6A, inset). Without maximizing the modulation contrast for each orientation by ensuring azimuthal polarization with a polarization rotator, there is very little modulation of the high-resolution information in the sample leading to a low signal-to-noise ratio in the SIM passbands. Reconstruction algorithms which use the standard Wiener filter approach will simply amplify the noise in the SIM passbands and yield an image which is essentially a standard TIRF image overlaid with hexagonal (or “honeycomb”) ringing artifacts (Figure 6A, right panel). A possible enhancement might be the use of iterative^{29,30} or blind reconstruction algorithms^{31,32} to reduce these artifacts depending on the type of sample. We recommend the use of the ImageJ plugin SIMcheck to check the quality of SIM data before and after reconstruction³³.

Figure 1: Layout of the multicolor TIRF-SIM setup. The TIRF-SIM microscope consists of three main parts, the beam generation unit, the pattern projection unit, and the detection unit. In the beam generation unit, three different lasers are aligned onto the same beam path via dichroic mirrors (DM1 and DM2) and directed through four optical elements for polarization control. First, a polarizer (P) ensures the purity of the linear polarization state of each of the laser beams. The following three optical elements are needed to rotate the polarization in a fast, automated manner as described in detail in the text. Afterwards, two lenses (L1 and L2) in a telescope configuration expand the beam to match the active surface of the spatial light modulator (SLM) and are diffracted into three beamlets by the SLM’s projected binary grating patterns (examples are shown in tiles 1-9). The polarization state of the illumination light relative to the SLM pattern is shown as an arrow. A second telescope (L3 and L4) de-magnifies the pattern and offers access to the Fourier plane of the SLM pattern. In this plane a spatial mask (SM) is used to filter out the central component and other unwanted diffraction components from the pixelated structure of the SLM and its internal wiring. Before the two remaining beams are focused onto the back focal plane of the objective (OB) via the tube lens (L5), two dichroic mirrors (DM3 and DM4) are included in the setup. DM4 acts as a conventional dichroic mirror in fluorescence microscopy to separate illumination from emission light. However, this mirror unavoidably induces ellipticity in the polarization state of the illumination light which can be compensated for by DM3, a dichroic mirror from ideally the same batch as DM4. The oil immersion TIRF objective has a large enough NA to directly launch two counter-propagating waves onto the coverslip that are reflected totally and give rise to a structured evanescent field in the coverslip. The sample is mounted on an x-y-z translation stage. Detection is performed through the same objective and DM4 in transmission, plus an additional filtering by bandpass emission filters, mounted in a computer controlled filter wheel (EFW). Finally, the image is projected onto a sCMOS camera by the internal microscope tube lens (L6).

Figure 2: Alignment of overlapping beams. (A) An SLM grating pattern windowed with a circular aperture is useful for alignment. If two non-overlapping beams are visible on the camera (left), then the position of the sample plane must be repositioned by iteratively adjusting the axial positions of the objective lens and the camera to give a single circular illumination spot (right). The beams must overlap in order to produce the sinusoidal excitation pattern required for TIRF-SIM. If the beams do not fully overlap this reduces the

field of view over which the interference pattern is formed. (B and C) The precise angle of incidence of the beams is important for TIRF-SIM. If the angle is incorrect, one of the beams will not be at the required angle for TIRF and this is easily visible when imaging a fluorescent dye solution. One beam has an angle of incidence greater than the critical angle which yields the circular spot, and the other does not, which leads to the bright streak on the left of the image in (B). (D) Adjusting the angle of mirror DM3 ensures both beams are incident at the same angle, and this can be validated by defocusing the objective: if correctly aligned, the xz projection of a z stack of a fluorescent dye sample should show two symmetrically intersecting beams with negligible background at the focus.

Figure 3: Synchronization dependencies of the different system components. (A) For fast SIM acquisition, synchronization of the system components using a hardware based solution is essential. (B) A data acquisition board (DAQ) should be used as a master trigger. A TTL signal from the DAQ board is sent to the sCMOS External Input and used to trigger the camera exposure. The camera Global Exposure output then triggers the SLM to display a grating pattern, and the SLM LED Enable output is used to digitally modulate the laser excitation such that the laser is only emitting when the SLM pixels are in the “on” state. After the exposure is complete, the camera Global Exposure output is used to advance the SLM pattern on to the next grating phase or angle. The DAQ board also outputs an analog voltage to the LCVR controller to control the linear polarization state of the illumination beam. This voltage is switched after acquisition of the 3 phase images for each pattern angle. After acquisition of 9 images for a single wavelength, the DAQ board outputs a signal to the emission filter wheel controller, and switches to the next wavelength. The DAQ board also applies a z -offset to the sample by outputting an analog voltage to the z -stage piezo controller.

Figure 4: TIRF-SIM imaging of test samples of 100 nm multicolor beads and fluorescently labelled amyloid fibrils. (A and B) Comparison of standard TIRF compared to TIRF-SIM reconstructions for 488 nm and 640 nm excitation. (C) Histogram of full-width half-maximum (FWHM) of Gaussian fits to the TIRF-SIM beads showing the expected resolution improvement. (D) TIRF versus TIRF-SIM of β -amyloid fibrils labelled with 10% rhodamine derivative dye (488 nm excitation). Scale bars 1 μm .

Figure 5: Live cell TIRF-SIM imaging. Comparison of conventional TIRF and TIRF-SIM images of (A, B) microtubules (emGFP-tubulin) in a HEK293 cell, (C, D) filamentous actin (LifeAct-GFP) in a COS-7 cell and (E, F) cytosolic GFP in a HEK293 cell. Images in B and F are single time points from the movies. Boxed areas are shown magnified in (G, H). Scale bars 3 μm .

Figure 6: Influence of polarization rotator on reconstructed bead images. (A) Without the use of a polarization rotator such as an LCVR, the signal-to-noise ratio in the SIM passbands is low which results in characteristic hexagonal artifacts in the reconstructed SIM images (right), (B) In 2D-SIM, the structured illumination patterns are directly visible in the Fourier transform of the raw images (left, excitation spatial frequency highlighted) as they fall within the radius of the emission OTF support, however in TIRF-SIM, they are outside the OTF support and therefore not visible (right). In this case, the pattern modulation contrast must be assessed using a sparse bead monolayer, as outlined in the protocol.

Figure 7: Spatial light modulator based pattern generation allows implementation of other imaging modalities such as multifocal SIM. (A) In MSIM, a lattice of square points

displayed on the SLM (inset) yields a lattice of diffraction limited foci at the image plane. A thin layer of low concentration rhodamine 6G is imaged to visualize the foci. The pattern is translated across the sample (B) and the acquired raw image z-stack is reconstructed to generate an image with reduced out-of-focus light (C). Scale bars 5 μm .

Animated Figure 1: Time series movie of emGFP-tubulin in a HEK293 cell. Rapid polymerization and depolymerization of emGFP labelled microtubules can be observed using TIRF-SIM. Images acquired using 50 ms exposure time per raw frame (450 ms per SIM frame) spaced at intervals of 0.5 s. Exposure time used was limited by the brightness of the fluorophore, not by the speed of the camera or SLM.

Animated Figure 2: Time series movie of cytosolic GFP in a HEK293 cell. Samples with low contrast such as this are not ideal samples for TIRF-SIM imaging. Retrograde membrane flow can be seen in the TIRF images but TIRF-SIM does not provide any additional information apart from at the cell edges. TIRF-SIM images were acquired using 50 ms exposure time per raw frame (450 ms per SIM frame) spaced at intervals of 5 s.

Supplemental Code File: Example SLM repertoire file (48449 300us 1-bit Balanced.seq3).

Supplemental Code File: Example SLM repertoire file (period9_001.bmp).

Supplemental Code File: Example SLM repertoire file (period9_002.bmp).

Supplemental Code File: Example SLM repertoire file (period9_003.bmp).

Supplemental Code File: Example SLM repertoire file (period9_004.bmp).

Supplemental Code File: Example SLM repertoire file (period9_005.bmp).

Supplemental Code File: Example SLM repertoire file (period9_006.bmp).

Supplemental Code File: Example SLM repertoire file (period9_007.bmp).

Supplemental Code File: Example SLM repertoire file (period9_008.bmp).

Supplemental Code File: Example SLM repertoire file (period9_009.bmp).

Supplemental Code File: Example SLM repertoire file (period9_mask_1.bmp).

Supplemental Code File: Example SLM repertoire file (period9_mask_2.bmp).

Supplemental Code File: Example SLM repertoire file (period9_mask_3.bmp).

Supplemental Code File: Example SLM repertoire file (TIRF-SIM_example.rep).

Supplemental Code File: Example grating generation code (1 of 2) (generate_gratings.m).

Supplemental Code File: Example grating generation code (2 of 2) (circular_mask.m).

Supplemental Code File: Example code to calculate modulation contrast (calculate_contrast.m).

DISCUSSION:

Custom-built TIRF-SIM systems such as the setup detailed in this protocol are capable of multicolor super-resolution imaging at high speed compared to commercially available microscopes. The inherent advantage of SIM as a super-resolution technique is that the temporal resolution is not limited by the photophysics of the fluorophore, compared to other methods such as single molecule localization microscopy (SMLM) or point scanning methods such as stimulated emission depletion microscopy (STED). Unlike these other techniques, SIM does not require photoswitchable or depletable fluorophores so multicolor imaging is straightforward. Non TIRF-SIM systems, such as optical sectioning SIM and multifocal SIM can usually achieve resolution improvements of 1.7 times or less in practice as opposed to the factor of 2 improvement reported here, and commercial systems are also often slower and less flexible than the system presented in this protocol.

The two main difficulties in implementing this technique are firstly the necessity for precise positioning of the six SIM beams within the TIR zone of the objective's back aperture, which requires a laborious and time consuming optical alignment procedure. Secondly, to produce high pattern contrast at the sample, polarization rotation is essential. For low NA 2D-SIM systems, polarization rotation can be avoided by careful choice of the linear polarization orientation, but this becomes impossible for TIRF-SIM²⁵. For high-speed multicolor imaging, electro-optical polarization control is necessary and this increases the complexity and expense of the system.

Limitations of the technique

TIRF-SIM, like conventional TIRF, is naturally limited to observation of biological structures and processes located at the basal cell membrane that can be illuminated by the 150-200 nm penetration depth of the evanescent field. While SIM is often quoted as being less photodamaging to cells than either STED or SMLM, lateral resolution doubling does still increase the required number of photons by at least 4-fold⁵ compared to conventional TIRF microscopy. For imaging at high frame rates with short exposures times, this photon increase necessitates use of increased illumination intensities. While any fluorophore may be used for SIM imaging of fixed or slow moving samples, high brightness fluorescent proteins or next generation synthetic dyes with enhanced photostability are recommended for live cell imaging.

Although this implementation is capable of imaging a single color at SIM frame rates in excess of 20 Hz, multicolor imaging in the presented system is limited by the switching time of the motorized emission filter wheel. Due to the large size of the sCMOS camera chip, the use of a multiband emission filter and image splitting optics would be possible and permit simultaneous imaging with multiple wavelengths at no speed penalty. Another possibility would be to alternate the different excitation lasers and use a multiband notch filter to reject the excitation light. The use of a binary ferroelectric SLM in this implementation also is not optimal. The diffraction efficiency of such an SLM is very low, so most of the incident light is in the zero order reflection, which is filtered out by the spatial mask. For applications requiring very high frame rates, the imaging speed is therefore limited by the output power of the laser diodes. The SLM also introduces some ellipticity in the polarization for wavelengths away from the 550 nm design wavelength where the pixels do not operate as ideal half wave plates. Although this could be compensated for by using an additional LCVR, the ideal solution may be the use of a digital micro-mirror device (DMD) as a pattern generator.

Possible modifications

The setup presented here is flexible and more easily modified than commercial instruments so other imaging modalities such as 3D-SIM, fast 2D-SIM, multifocal SIM (MSIM) and non-linear SIM (NL-SIM) can be implemented^{21,34,35}.

2D-SIM can be well suited for imaging relatively flat, fast moving structures such as the peripheral endoplasmic reticulum. The peripheral ER lies deeper within the cell than can be illuminated using a TIRF evanescent field but due to its flat structure can be imaged using standard 2D-SIM with negligible out-of-focus background. Additionally, the use of improved optical sectioning reconstruction algorithms to suppress out-of-focus light extend the use of 2D-SIM to optically thick samples, albeit where axial resolution doubling is not required²¹.

In MSIM, the sample is illuminated by a sparse lattice of excitation foci³⁶. This modality can be implemented by simply removing the spatial mask (SM) and replacing it by a polarizer. The SLM now operates as an amplitude modulator. The binary SIM gratings displayed on the SLM can be replaced by a 2D lattice of spots, with the size of the spots chosen to be equal to the size of a diffraction limited focus in the image plane. In Figure 7A, a lattice of 4x4 pixel squares is displayed on the SLM (inset) which when demagnified onto the sample generates diffraction limited foci of 150 x 150 nm, given the physical SLM pixel size of 13.62 μm . The excitation foci can then be translated by shifting the lattice pattern on the SLM and this is repeated multiple times in order to illuminate the entire field of view. Images are acquired for each translated pattern position and the stack is post-processed to yield a reconstructed image with improved resolution of up to a factor of $\sqrt{2}$ and reduced out-of-focus light compared to the equivalent widefield image³⁰. This modality can be useful for imaging thick, dense samples for which standard SIM is unsuited, for example low contrast structures such as stained red blood cells (Figure 7C), although the acquisition time is increased due to the large number of raw frames required per field of view (in this case $N = 168$).

Finally, the setup can be modified to enable either high-NA linear TIRF-SIM or patterned activation non-linear SIM (PA NL-SIM), as presented recently by Li *et al*, by use of an ultrahigh 1.7 NA objective or addition of a 405 nm photoactivation laser and careful optimization of the SLM grating patterns³⁵.

Future Applications

SIM is still a rapidly evolving technique and many applications in the life sciences will be enabled in the future. The speed, resolution, and contrast enhancements of the technique and the capability of using standard fluorophores mean that for bioimaging, SIM is set to replace conventional many microscope systems, such as confocal and wide field platforms.

Commercial SIM systems are already available today with outstanding technical specifications, however, they are beyond the financial reach of many research laboratories, and, crucially, they are inflexible to be modified and developed to implement the latest research developments in the field. They also lack the essential capability to 'be adapted for the experiment at hand', often a critical bottleneck in cutting edge life science research. The system described here will be particularly well suited to study dynamic processes near the cell surface, for *in vitro* studies of reconstituted bilayer systems, to study surface chemistry in the materials and physical sciences, e.g. of 2D materials, and many other applications.

ACKNOWLEDGMENTS:

This work was supported by grants from the Leverhulme Trust, the Engineering and Physical

Sciences Research Council [EP/H018301/1, EP/G037221/1]; Alzheimer Research UK [ARUK-EG2012A-1]; Wellcome Trust [089703/Z/09/Z] and Medical Research Council [MR/K015850/1, MR/K02292X/1]. We thank E. Avezov and M. Lu for transfection of the LifeAct-GFP and cytosolic-GFP cells respectively, and W. Chen for preparation of the HEK293 culture. We also thank K. O'Holleran for assistance with the design of the microscope, and L. Shao and R. Heintzmann for useful discussions and suggestions.

DISCLOSURES:

The authors have nothing to disclose.

REFERENCES:

1. Heintzmann, R. & Cremer, C. G. Laterally modulated excitation microscopy: improvement of resolution by using a diffraction grating. *BiOS Eur.* **3568**, 185–196, doi:10.1117/12.336833 (1999).
2. Gustafsson, M. G. L. Surpassing the lateral resolution limit by a factor of two using structured illumination microscopy. *J. Microsc.* **198** (2), 82–87, doi:10.1046/j.1365-2818.2000.00710.x (2000).
3. Shim, S.-H. *et al.* Super-resolution fluorescence imaging of organelles in live cells with photoswitchable membrane probes. *Proc. Natl. Acad. Sci. U. S. A.* **109** (35), 13978–13983, doi:10.1073/pnas.1201882109 (2012).
4. Urban, N. T., Willig, K. I., Hell, S. W. & Nägerl, U. V. STED Nanoscopy of Actin Dynamics in Synapses Deep Inside Living Brain Slices. *Biophys. J.* **101** (5), 1277–1284, doi:10.1016/j.bpj.2011.07.027 (2011).
5. Liu, Z., Lavis, L. D. & Betzig, E. Imaging Live-Cell Dynamics and Structure at the Single-Molecule Level. *Mol. Cell* **58** (4), 644–659, doi:10.1016/j.molcel.2015.02.033 (2015).
6. Westphal, V. *et al.* Video-Rate Far-Field Optical Nanoscopy Dissects Synaptic Vesicle Movement. *Science* (80-.). **320** (5873), 246–249, doi:10.1126/science.1154228 (2008).
7. Davies, T. *et al.* CYK4 Promotes Antiparallel Microtubule Bundling by Optimizing MKLP1 Neck Conformation. *PLOS Biol.* **13** (4), e1002121, doi:10.1371/journal.pbio.1002121 (2015).
8. Laine, R. F. *et al.* Structural analysis of herpes simplex virus by optical super-resolution imaging. *Nat. Commun.* **6**, 5980, doi:10.1038/ncomms6980 (2015).
9. Pinotsi, D. *et al.* Direct observation of heterogeneous amyloid fibril growth kinetics via two-color super-resolution microscopy. *Nano Lett.* **14** (1), 339–45, doi:10.1021/nl4041093 (2014).
10. Esbjörner, E. K. *et al.* Direct observations of amyloid β Self-assembly in live cells provide insights into differences in the kinetics of A β (1-40) and A β (1-42) aggregation. *Chem. Biol.* **21** (6), 732–742, doi:10.1016/j.chembiol.2014.03.014 (2014).
11. Michel, C. H. *et al.* Extracellular monomeric tau protein is sufficient to initiate the spread of tau protein pathology. *J. Biol. Chem.* **289** (2), 956–967, doi:10.1074/jbc.M113.515445 (2014).
12. Pinotsi, D., Kaminski Schierle, G. S. & Kaminski, C. F. Optical Super-Resolution Imaging of β -Amyloid Aggregation In Vitro and In Vivo: Method and Techniques. *Syst. Biol. Alzheimer's Dis. SE - 6* **1303**, 125–141, doi:10.1007/978-1-4939-2627-5_6 (2016).
13. Axelrod, D. Cell-substrate contacts illuminated by total internal reflection fluorescence. *J. Cell Biol.* **89** (1), 141–145, doi:10.1083/jcb.89.1.141 (1981).

14. Cragg, G. E. & So, P. T. Lateral resolution enhancement with standing evanescent waves. *Opt. Lett.* **25** (1), 46–48 (2000).
15. Chung, E., Kim, D. & So, P. T. Extended resolution wide-field optical imaging: objective-launched standing-wave total internal reflection fluorescence microscopy. *Opt. Lett.* **31** (7), 945, doi:10.1364/OL.31.000945 (2006).
16. Kner, P., Chhun, B. B., Griffis, E. R., Winoto, L. & Gustafsson, M. G. L. Super-resolution video microscopy of live cells by structured illumination. *Nat. Methods* **6** (5), 339–42, doi:10.1038/nmeth.1324 (2009).
17. Fiolka, R., Shao, L., Rego, E. H., Davidson, M. W. & Gustafsson, M. G. L. Time-lapse two-color 3D imaging of live cells with doubled resolution using structured illumination. *Proc. Natl. Acad. Sci. U. S. A.* **109** (14), 5311–5, doi:10.1073/pnas.1119262109 (2012).
18. Brunstein, M., Wicker, K., Héroult, K., Heintzmann, R. & Oheim, M. Full-field dual-color 100-nm super-resolution imaging reveals organization and dynamics of mitochondrial and ER networks. *Opt. Express* **21** (22), 26162–26173, doi:10.1364/OE.21.026162 (2013).
19. Förster, R. *et al.* Simple structured illumination microscope setup with high acquisition speed by using a spatial light modulator. *Opt. Express* **22** (17), 20663, doi:10.1364/OE.22.020663 (2014).
20. Lu-Walther, H.-W. *et al.* fastSIM: a practical implementation of fast structured illumination microscopy. *Methods Appl. Fluoresc.* **014001**, 14001, doi:10.1088/2050-6120/3/1/014001 (2015).
21. Shaw, M., Zajiczek, L. & O'Holleran, K. High speed structured illumination microscopy in optically thick samples. *Methods*, doi:10.1016/j.ymeth.2015.03.020 (2015).
22. Olshausen, P. von Total internal reflection microscopy: super-resolution imaging of bacterial dynamics and dark field imaging. PhD dissertation, University of Freiburg (2012).
23. Gustafsson, M. G. L. *et al.* Three-dimensional resolution doubling in wide-field fluorescence microscopy by structured illumination. *Biophys. J.* **94** (12), 4957–70, doi:10.1529/biophysj.107.120345 (2008).
24. Meadowlark Optics Inc *Basic Polarization Techniques and Devices*. (2005).
25. O'Holleran, K. & Shaw, M. Polarization effects on contrast in structured illumination microscopy. *Opt. Lett.* **37** (22), 4603, doi:10.1364/OL.37.004603 (2012).
26. Brankner, S. Z. & Hobson, M. *Synchronization and Triggering with the ORCA-Flash4.0 Scientific CMOS Camera*. at <http://www.hamamatsu.com/resources/pdf/sys/SCAS0098E_synchronization.pdf> (2013).
27. Gustafsson, M. G. L. *et al.* Three-dimensional resolution doubling in wide-field fluorescence microscopy by structured illumination. *Biophys. J.* **94** (12), 4957–70, doi:10.1529/biophysj.107.120345 (2008).
28. Wicker, K. Non-iterative determination of pattern phase in structured illumination microscopy using auto-correlations in Fourier space. *Opt. Express* **21** (21), 24692, doi:10.1364/OE.21.024692 (2013).
29. Boulanger, J., Pustelnik, N. & Condat, L. Non-smooth convex optimization for an efficient reconstruction in structured illumination microscopy. *2014 IEEE 11th Int. Symp. Biomed. Imaging* **3** (1), 995–998, doi:10.1109/ISBI.2014.6868040 (2014).
30. Ströhl, F. & Kaminski, C. F. A joint Richardson—Lucy deconvolution algorithm for the reconstruction of multifocal structured illumination microscopy data. *Methods Appl. Fluoresc.* **3** (1), 014002, doi:10.1088/2050-6120/3/1/014002 (2015).

31. Mudry, E. *et al.* Structured illumination microscopy using unknown speckle patterns. *Nat. Photonics* **6** (5), 312–315, doi:10.1038/nphoton.2012.83 (2012).
32. Ayuk, R. *et al.* Structured illumination fluorescence microscopy with distorted excitations using a filtered blind-SIM algorithm. *Opt. Lett.* **38** (22), 4723, doi:10.1364/OL.38.004723 (2013).
33. Ball, G. *et al.* SIMcheck: a Toolbox for Successful Super-resolution Structured Illumination Microscopy. *Sci. Rep.* **5**, 15915, doi:10.1038/srep15915 (2015).
34. York, A. G. *et al.* Resolution doubling in live, multicellular organisms via multifocal structured illumination microscopy. *Nat. Methods* **9** (7), 749–754, doi:10.1038/nmeth.2025 (2012).
35. Li, D. *et al.* Extended-resolution structured illumination imaging of endocytic and cytoskeletal dynamics. *Science* **349** (6251), aab3500–aab3500, doi:10.1126/science.aab3500 (2015).
36. York, A. G. *et al.* Resolution doubling in live, multicellular organisms via multifocal structured illumination microscopy. *Nat. Methods* **9** (7), 749–54, doi:10.1038/nmeth.2025 (2012).

Figure 1: Layout of the multicolor TIRF-SIM setup

[Click here to download Figure figure1.png](#)

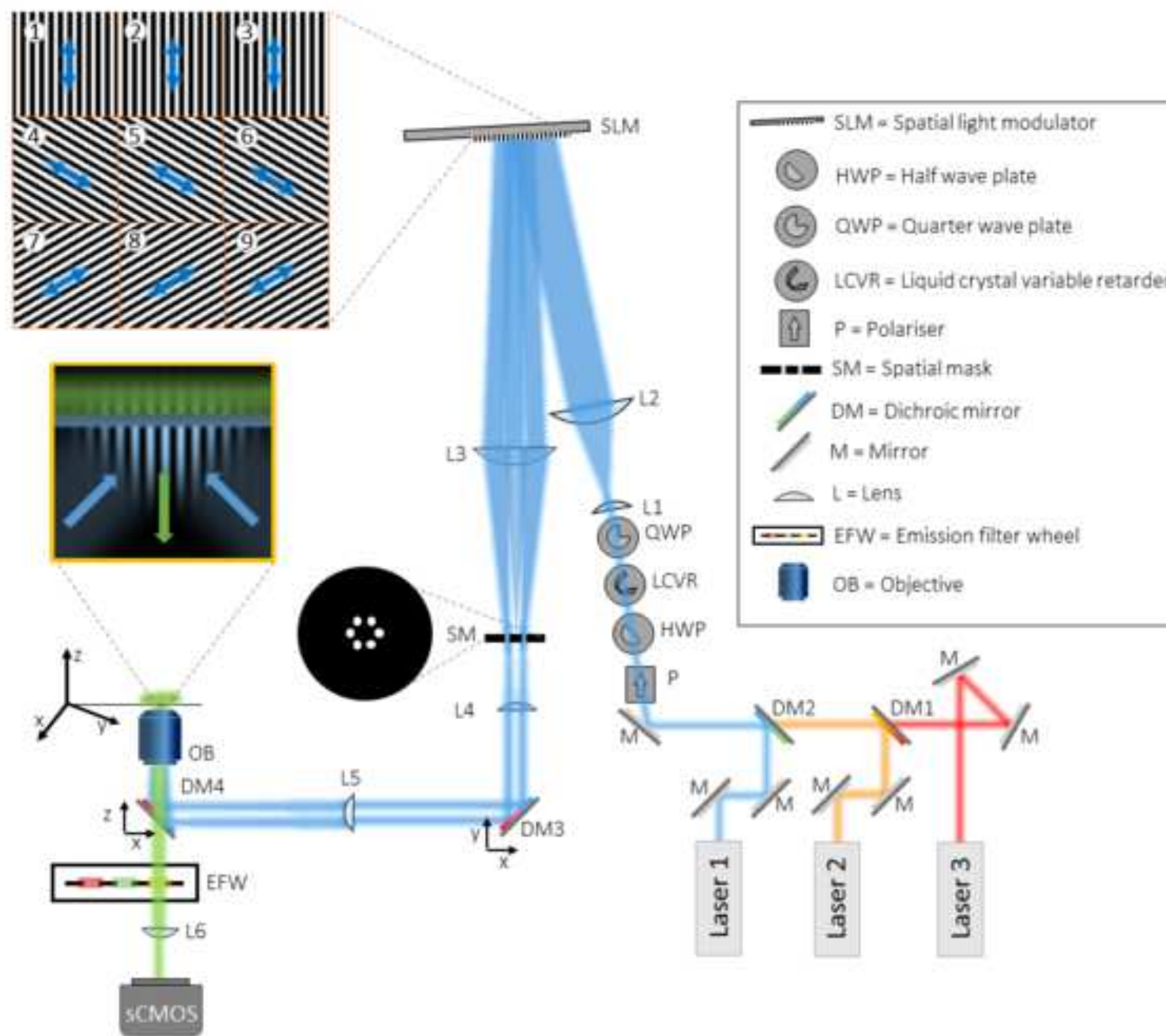
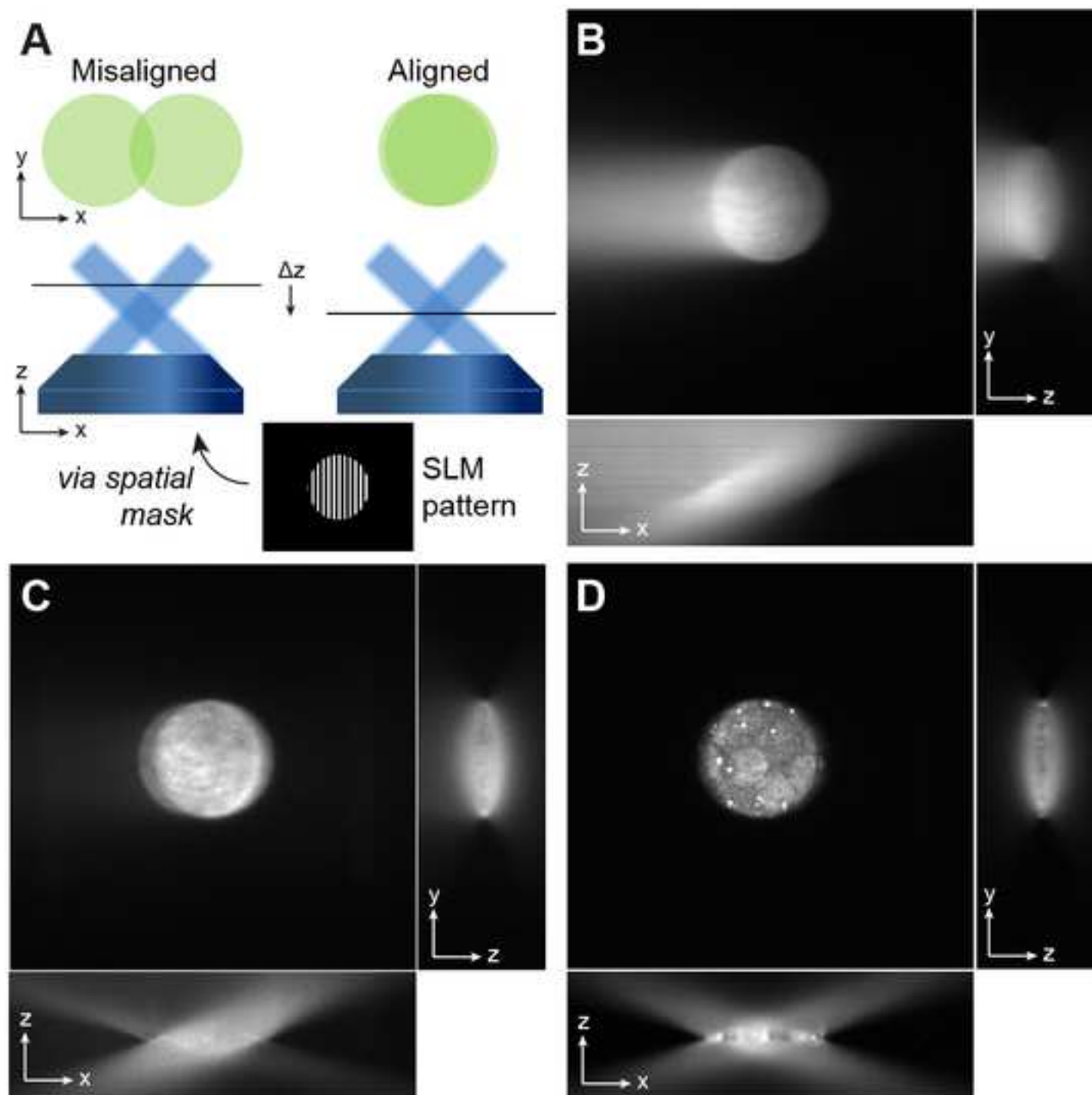


Figure 2: Alignment of overlapping beams.

[Click here to download Figure figure2.png](#)



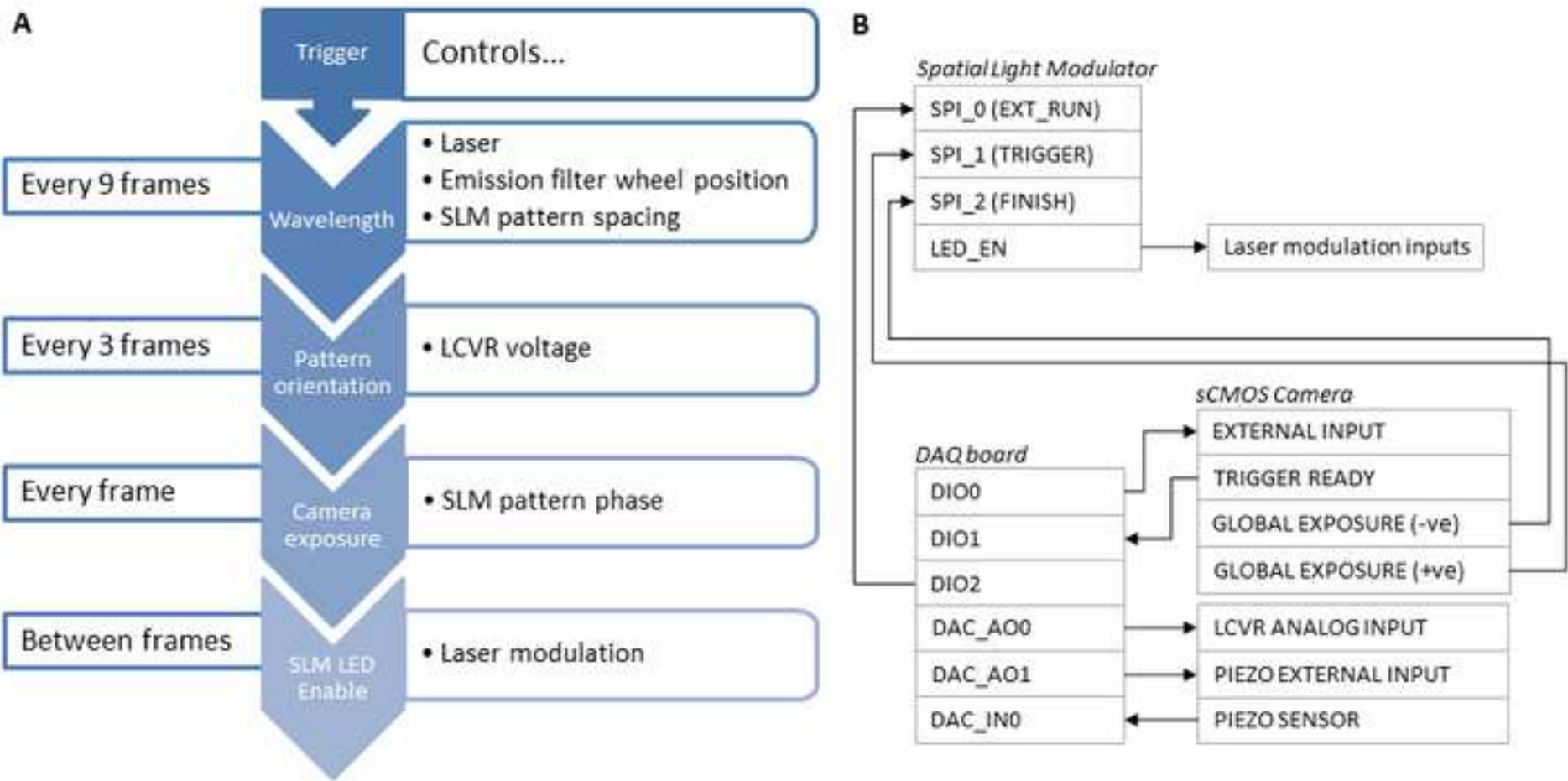
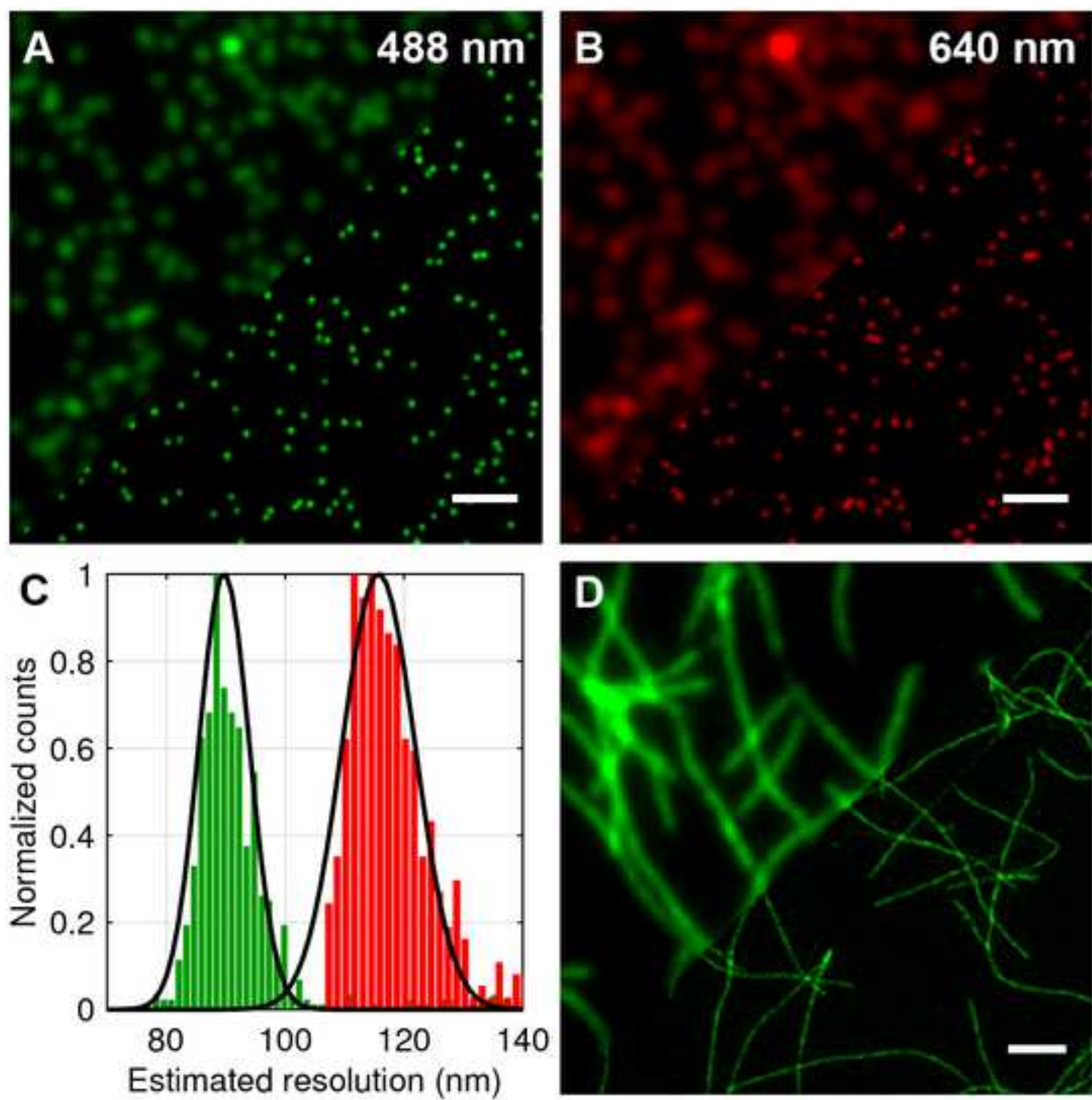


Figure 4: TIRF-SIM imaging of test samples of 100 nm multicolor beads and fluorescently labelled amyloid fibrils.

[Click here to download Figure figure4.png](#)



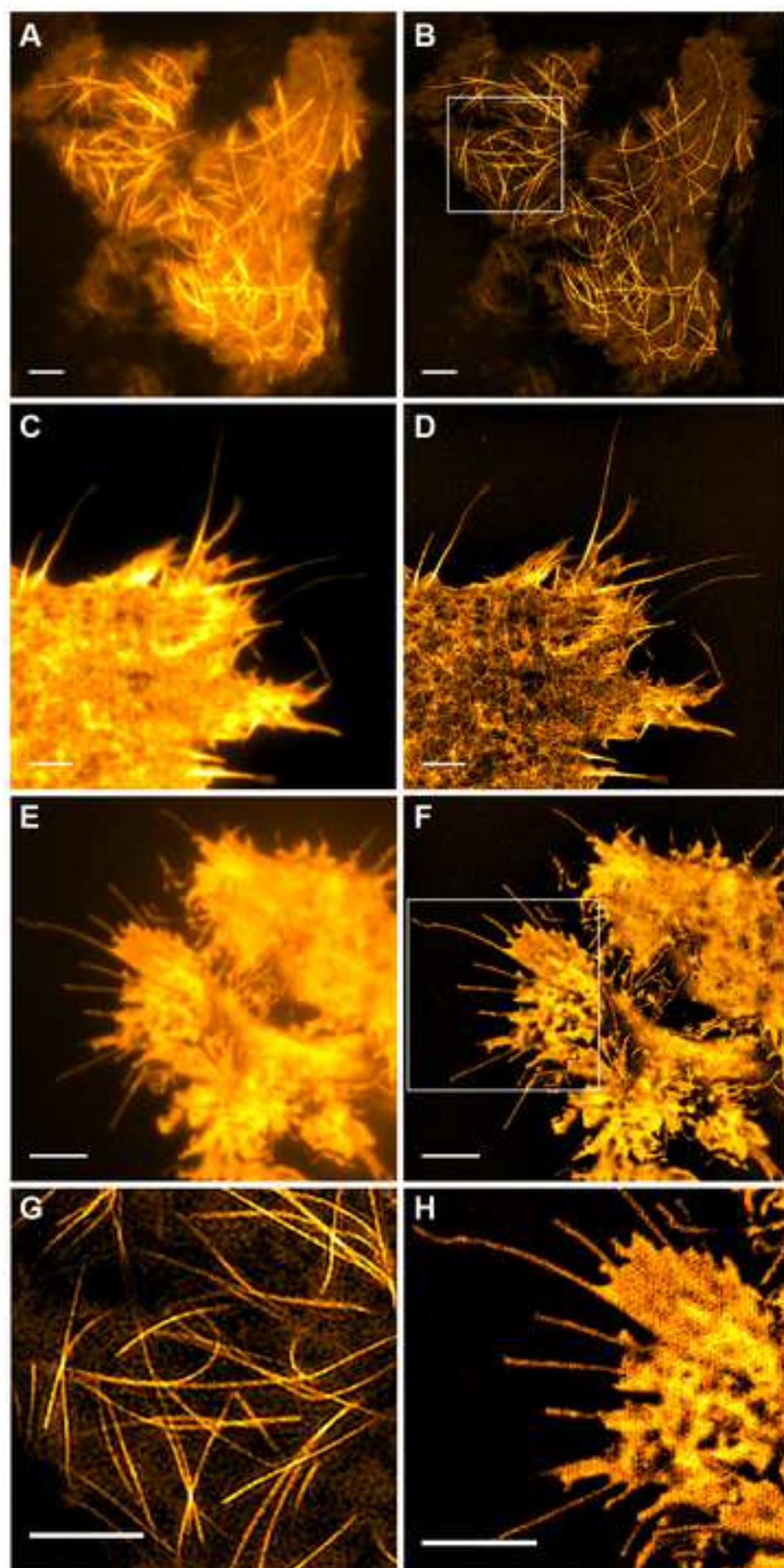
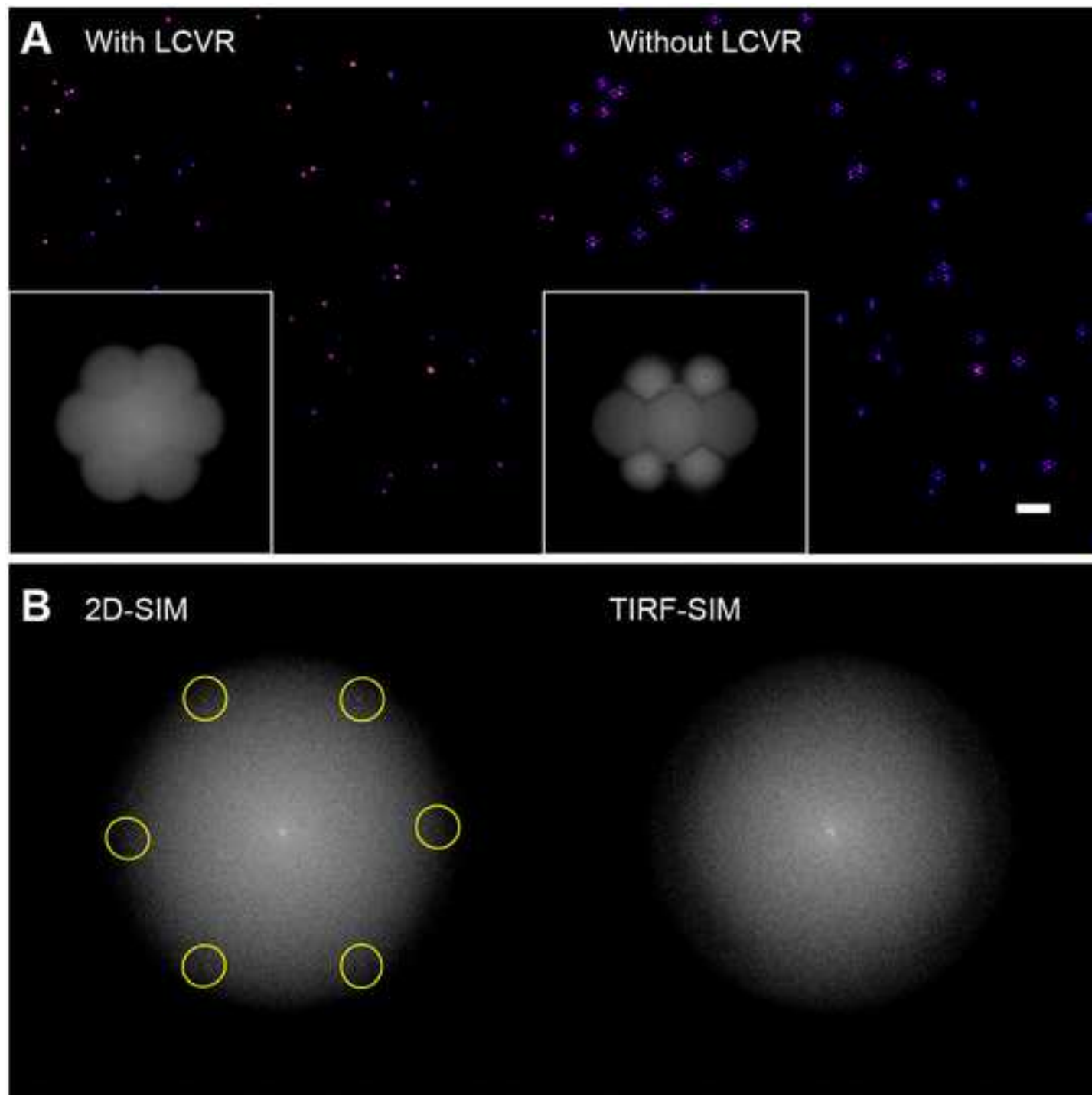
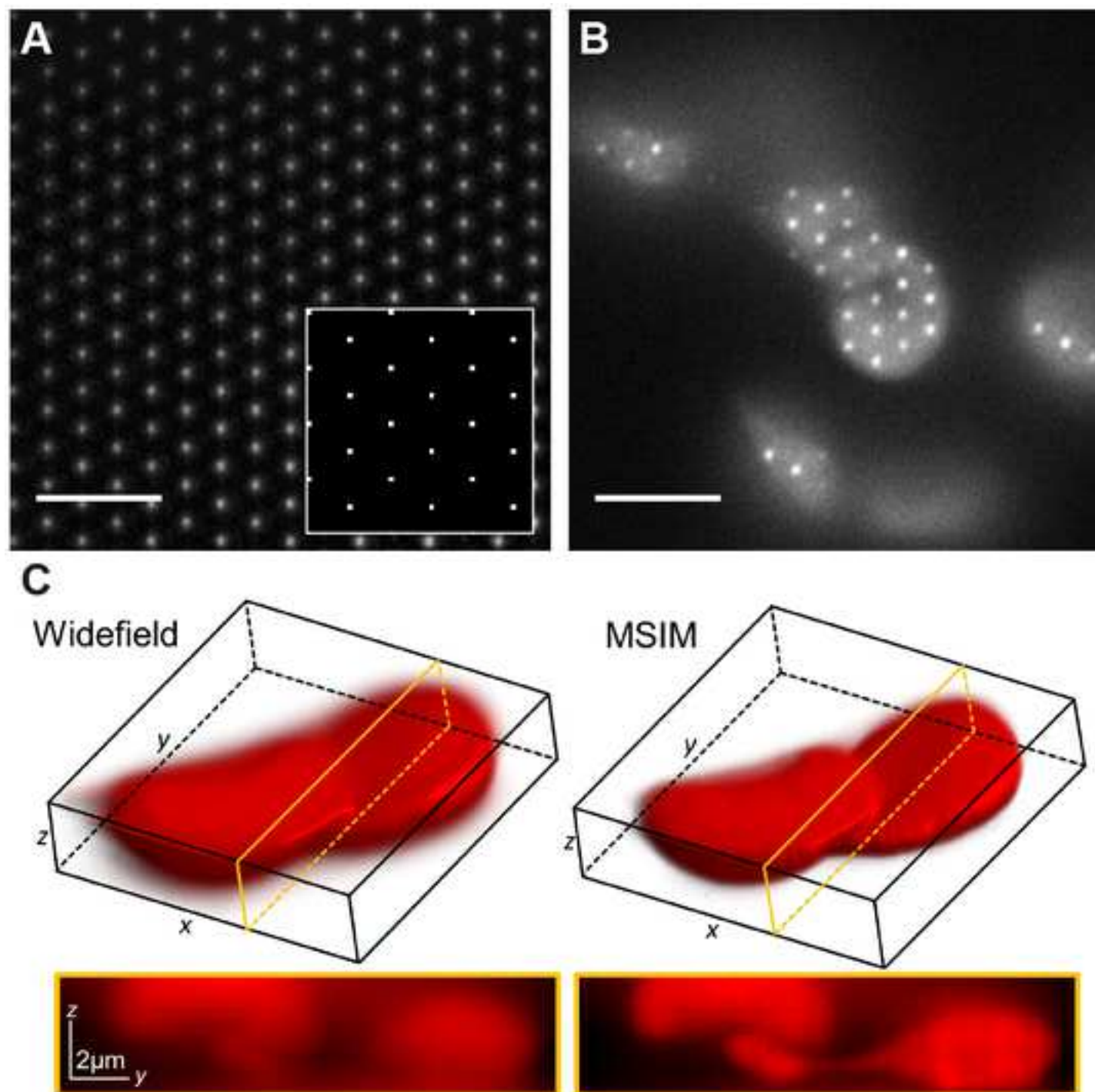


Figure 6: Influence of polarization rotator on reconstructed bead images.

[Click here to download Figure figure6.png](#)





Name of Reagent/ Equipment	Company	Catalog Number
488 nm laser	Toptica	iBeam SMART
561 nm laser	Coherent	OBIS LS
640 nm laser	Cobolt	MLD
Long-pass dichroic mirrors	Thorlabs	
Quad band dichroic mirror	Chroma	ZT405/488/561/640rpc
Quad band dichroic mirror	Chroma	ZT405/488/561/640rpc
1" square kinematic mount	Edmund Optics	58-860
Glan-Taylor calcite polarizers	Thorlabs	GT5-A
Glan-Taylor mount	Thorlabs	SM05PM5
Achromatic half wave plate	Thorlabs	AHWP05M-600
Rotation cage mount	Thorlabs	CRM1/M
Liquid Crystal Variable Retarder	Meadowlark Optics	SWIFT
LCVR controller	Meadowlark Optics	D3060HV
Achromatic quarter wave plate	Meadowlark Optics	AQM-100-0545
Rotation cage mount	Thorlabs	CRM1P/M
10 mm achromatic doublet	Thorlabs	AC080-010-A-ML
200 mm achromatic doublet	Thorlabs	AC254-200-A-ML
Cage XY Translators	Thorlabs	CXY1
	Forth Dimension	
Ferroelectric spatial light modulator	Displays	M0787-00249
	Forth Dimension	
SLM mounting frame	Displays	M0787-10014
Ø50.8 mm Gimbal Mirror Mount	Thorlabs	GM200/M
Two-Axis Linear Translation Stage with		
Rotating Platform	Thorlabs	XYR1/M
Rail carrier	Newport	M-PRC-3
Precision Optical Rail	Newport	PRL-6
300 mm achromatic doublet lens	Qioptiq	G322 273 322
140 mm achromatic doublet lens	Qioptiq	G322 239 322
Precision XY Translation Mounts	Thorlabs	LM2XY
Lens Mounting Adapters	Thorlabs	SM2AD32
Translation stages	Comar	12XT65

XY Translator with Differential Drives	Thorlabs	ST1XY-D/M
Rotation cage mount	Thorlabs	CRM1/M
300 mm achromatic doublet	Thorlabs	AC508-300-A-ML
Automated XY stage with Z-piezo top plate	ASI	PZ-2150-XYFT-PZ-IX71
Inverted microscope frame	Olympus	IX-71
Objective lens	Olympus	UAPON100XOTIRF
High speed filter wheel	Prior Scientific	HF110A
Bandpass emission filters	Semrock	FF01-525/30, FF01-676/29
sCMOS camera	Hamamatsu	ORCA Flash v4.0
Stage top incubator	OKO Lab	H301-K-FRAME
Stainless steel optical posts	Thorlabs	TR series
Post holders	Thorlabs	PH series
Kinematic mirror mounts	Thorlabs	KM100
Shearing interferometer	Thorlabs	SI100
100 nm fluorescent microspheres	Life Technologies	T-7279
Rhodamine 6G	Sigma Aldrich	83697-250MG
8 well glass bottom dishes	ibidi	80827
	Thermo Fisher	
Nunc Lab-Tek II Chambered Coverglass	Scientific	155409
0.01mm microscope reticle slide	EMS	68039-22
	Thermo Fisher	
CellLight Tubulin-GFP, BacMam 2.0	Scientific	C10613

Comments/Description

with digital modulation

with digital modulation

with digital modulation

for combining excitation beams

3 mm thick, TIRF imaging flat, mounted in Olympus BX filter cube

From same batch as above, 25 x 25 mm

For alignment of LCVR

400 - 800 nm

For HWP

Custom built to provide full wave retardance over the range 488 to 640 nm.

Two channel high voltage controller for liquid crystal retarders

For QWP

For beam expander

For beam expander

SXGA-3DM (IFF) Microdisplay Type M249, 1280 x 1024 pixels, with driver board

Fixed to custom built aluminium mount

For SLM mounting

For SLM mounting

For SLM mounting

For SLM mounting

f = 300 mm, 31.5 mm diameter

f = 140 mm, 31.5 mm diameter

For mounting 31.5 mm lenses in 2" mounts

Dovetail, side drive

for spatial filter
for spatial filter
Excitation tube lens
with MS-2000 controller

100X/1.49NA
with Prior ProScan III controller

For live cell imaging, with Bold Line temperature and CO2 controllers
for mounting optical components
for mounting optical components
for mounting 1" mirrors

Tetraspeck

with #1.5 coverglass

with #1.5 coverglass



[Click here to access/download](#)

Animated Figure (video and/or .ai figure files)
movie1.mov





[Click here to access/download](#)

Animated Figure (video and/or .ai figure files)
movie2.mov



Title of Article:

Author(s):

Item 1 (check one box): The Author elects to have the Materials be made available (as described at <http://www.jove.com/publish>) via: ☒ Standard Access ☐ Open Access

Item 2 (check one box):

- ☒ The Author is NOT a United States government employee.
- ☐ The Author is a United States government employee and the Materials were prepared in the course of his or her duties as a United States government employee.
- ☐ The Author is a United States government employee but the Materials were NOT prepared in the course of his or her duties as a United States government employee.

ARTICLE AND VIDEO LICENSE AGREEMENT

1. Defined Terms. As used in this Article and Video License Agreement, the following terms shall have the following meanings: “**Agreement**” means this Article and Video License Agreement; “**Article**” means the article specified on the last page of this Agreement, including any associated materials such as texts, figures, tables, artwork, abstracts, or summaries contained therein; “**Author**” means the author who is a signatory to this Agreement; “**Collective Work**” means a work, such as a periodical issue, anthology or encyclopedia, in which the Materials in their entirety in unmodified form, along with a number of other contributions, constituting separate and independent works in themselves, are assembled into a collective whole; “**CRC License**” means the Creative Commons Attribution 3.0 Agreement, the terms and conditions of which can be found at: <http://creativecommons.org/licenses/by/3.0/us/legalcode>;

“**Derivative Work**” means a work based upon the Materials or upon the Materials and other pre-existing works, such as a translation, musical arrangement, dramatization, fictionalization, motion picture version, sound recording, art reproduction, abridgment, condensation, or any other form in which the Materials may be recast, transformed, or adapted; “**Institution**” means the institution, listed on the last page of this Agreement, by which the Author was employed at the time of the creation of the Materials; “**JoVE**” means MyJove Corporation, a Massachusetts corporation and the publisher of *The Journal of Visualized Experiments*;

“**Materials**” means the Article and / or the Video; “**Parties**” means the Author and JoVE; “**Video**” means any video(s) made by the Author, alone or in conjunction with any other parties, or by JoVE or its affiliates or agents, individually or in collaboration with the Author or any other parties, incorporating all or any portion of the Article, and in which the Author may or may not appear.

2. Background. The Author, who is the author of the Article, in order to ensure the dissemination and protection of the Article, desires to have the JoVE publish the Article and create and transmit videos based on the Article. In furtherance of such goals, the Parties desire to memorialize in this Agreement the respective rights of each Party in and to the Article and the Video.

3. Grant of Rights in Article. In consideration of JoVE agreeing to publish the Article, the Author hereby grants to JoVE, subject to **Sections 4 and 7** below, the exclusive, royalty-free, perpetual (for the full term of copyright in the Article, including any extensions thereto) license (a) to publish, reproduce, distribute, display and store the Article in all forms, formats and media whether now known or hereafter developed (including without limitation in print, digital and electronic form) throughout the world, (b) to translate the Article into other languages, create adaptations, summaries or extracts of the Article or other Derivative Works (including, without limitation, the Video) or Collective Works based on all or any portion of the Article and exercise all of the rights set forth in (a) above in such translations, adaptations, summaries, extracts, Derivative Works or Collective Works and

(c) to license others to do any or all of the above. The foregoing rights may be exercised in all media and formats, whether now known or hereafter devised, and include the right to make such modifications as are technically necessary to exercise the rights in other media and formats. If the “Open Access” box has been checked in **Item 1** above, JoVE and the Author hereby grant to the public all such rights in the Article and Video as provided in, but subject to all limitations and requirements set forth in, the CRC License.

4. Retention of Rights in Article. Notwithstanding the exclusive license granted to JoVE in **Section 3** above, the

ARTICLE AND VIDEO LICENSE AGREEMENT

Author shall, with respect to the Article, retain the non-exclusive right to use all or part of the Article for the non-commercial purpose of giving lectures, presentations or teaching classes, and to post a copy of the Article on the Institution's website or the Author's personal website, in each case provided that a link to the Article on the JoVE website is provided and notice of JoVE's copyright in the Article is included. All non-copyright intellectual property rights in and to the Article, such as patent rights, shall remain with the Author.

5. Grant of Rights in Video – Standard Access. This **Section 5** applies if the "Standard Access" box has been checked in **Item 1** above or if no box has been checked in **Item 1** above. In consideration of JoVE agreeing to produce, display or otherwise assist with the Video, the Author hereby acknowledges and agrees that, Subject to **Section 7** below, JoVE is and shall be the sole and exclusive owner of all rights of any nature, including, without limitation, all copyrights, in and to the Video. To the extent that, by law, the Author is deemed, now or at any time in the future, to have any rights of any nature in or to the Video, the Author hereby disclaims all such rights and transfers all such rights to JoVE.

6. Grant of Rights in Video – Open Access. This **Section 6** applies only if the "Open Access" box has been checked in **Item 1** above. In consideration of JoVE agreeing to produce, display or otherwise assist with the Video, the Author hereby grants to JoVE, subject to **Section 7** below, the exclusive, royalty-free, perpetual (for the full term of copyright in the Article, including any extensions thereto) license (a) to publish, reproduce, distribute, display and store the Video in all forms, formats and media whether now known or hereafter developed (including without limitation in print, digital and electronic form) throughout the world, (b) to translate the Video into other languages, create adaptations, summaries or extracts of the Video or other Derivative Works or Collective Works based on all or any portion of the Video and exercise all of the rights set forth in (a) above in such translations, adaptations, summaries, extracts, Derivative Works or Collective Works and (c) to license others to do any or all of the above. The foregoing rights may be exercised in all media and formats, whether now known or hereafter devised, and include the right to make such modifications as are technically necessary to exercise the rights in other media and formats.

7. Government Employees. If the Author is a United States government employee and the Article was prepared in the course of his or her duties as a United States government employee, as indicated in **Item 2** above, and any of the licenses or grants granted by the Author hereunder exceed the scope of the 17 U.S.C. 403, then the rights granted hereunder shall be limited to the maximum rights permitted under such statute. In such case, all provisions contained herein that are not in conflict with such statute shall remain in full force and effect, and all provisions contained herein that do so conflict

shall be deemed to be amended so as to provide to JoVE the maximum rights permissible within such statute.

8. Likeness, Privacy, Personality. The Author hereby grants JoVE the right to use the Author's name, voice, likeness, picture, photograph, image, biography and performance in any way, commercial or otherwise, in connection with the Materials and the sale, promotion and distribution thereof. The Author hereby waives any and all rights he or she may have, relating to his or her appearance in the Video or otherwise relating to the Materials, under all applicable privacy, likeness, personality or similar laws.

9. Author Warranties. The Author represents and warrants that the Article is original, that it has not been published, that the copyright interest is owned by the Author (or, if more than one author is listed at the beginning of this Agreement, by such authors collectively) and has not been assigned, licensed, or otherwise transferred to any other party. The Author represents and warrants that the author(s) listed at the top of this Agreement are the only authors of the Materials. If more than one author is listed at the top of this Agreement and if any such author has not entered into a separate Article and Video License Agreement with JoVE relating to the Materials, the Author represents and warrants that the Author has been authorized by each of the other such authors to execute this Agreement on his or her behalf and to bind him or her with respect to the terms of this Agreement as if each of them had been a party hereto as an Author. The Author warrants that the use, reproduction, distribution, public or private performance or display, and/or modification of all or any portion of the Materials does not and will not violate, infringe and/or misappropriate the patent, trademark, intellectual property or other rights of any third party. The Author represents and warrants that it has and will continue to comply with all government, institutional and other regulations, including, without limitation all institutional, laboratory, hospital, ethical, human and animal treatment, privacy, and all other rules, regulations, laws, procedures or guidelines, applicable to the Materials, and that all research involving human and animal subjects has been approved by the Author's relevant institutional review board.

10. JoVE Discretion. If the Author requests the assistance of JoVE in producing the Video in the Author's facility, the Author shall ensure that the presence of JoVE employees, agents or independent contractors is in accordance with the relevant regulations of the Author's institution. If more than one author is listed at the beginning of this Agreement, JoVE may, in its sole discretion, elect not take any action with respect to the Article until such time as it has received complete, executed Article and Video License Agreements from each such author. JoVE reserves the right, in its absolute and sole discretion and without giving any reason therefore, to accept or decline any work submitted to JoVE. JoVE and its employees, agents and independent contractors shall have full, unfettered access to the facilities of the Author or of the Author's institution as necessary to make the Video, whether actually published or not. JoVE has sole discretion as to the method of making and publishing the Materials, including,

ARTICLE AND VIDEO LICENSE AGREEMENT

without limitation, to all decisions regarding editing, lighting, filming, timing of publication, if any, length, quality, content and the like.

11. **Indemnification.** The Author agrees to indemnify JoVE and/or its successors and assigns from and against any and all claims, costs, and expenses, including attorney's fees, arising out of any breach of any warranty or other representations contained herein. The Author further agrees to indemnify and hold harmless JoVE from and against any and all claims, costs, and expenses, including attorney's fees, resulting from the breach by the Author of any representation or warranty contained herein or from allegations or instances of violation of intellectual property rights, damage to the Author's or the Author's institution's facilities, fraud, libel, defamation, research, equipment, experiments, property damage, personal injury, violations of institutional, laboratory, hospital, ethical, human and animal treatment, privacy or other rules, regulations, laws, procedures or guidelines, liabilities and other losses or damages related in any way to the submission of work to JoVE, making of videos by JoVE, or publication in JoVE or elsewhere by JoVE. The Author shall be responsible for, and shall hold JoVE harmless from, damages caused by lack of sterilization, lack of cleanliness or by contamination due to the making of a video by JoVE its employees, agents or independent contractors. All sterilization, cleanliness or decontamination procedures shall be solely the responsibility of the Author and shall be undertaken at the Author's expense. All indemnifications provided herein shall include JoVE's attorney's fees and costs related to said losses or

damages. Such indemnification and holding harmless shall include such losses or damages incurred by, or in connection with, acts or omissions of JoVE, its employees, agents or independent contractors.

12. **Fees.** To cover the cost incurred for publication, JoVE must receive payment before production and publication the Materials. Payment is due in 21 days of invoice. Should the Materials not be published due to an editorial or production decision, these funds will be returned to the Author. Withdrawal by the Author of any submitted Materials after final peer review approval will result in a US\$1,200 fee to cover pre-production expenses incurred by JoVE. If payment is not received by the completion of filming, production and publication of the Materials will be suspended until payment is received.

13. **Transfer, Governing Law.** This Agreement may be assigned by JoVE and shall inure to the benefits of any of JoVE's successors and assignees. This Agreement shall be governed and construed by the internal laws of the Commonwealth of Massachusetts without giving effect to any conflict of law provision thereunder. This Agreement may be executed in counterparts, each of which shall be deemed an original, but all of which together shall be deemed to be one and the same agreement. A signed copy of this Agreement delivered by facsimile, e-mail or other means of electronic transmission shall be deemed to have the same legal effect as delivery of an original signed copy of this Agreement.

A signed copy of this document must be sent with all new submissions. Only one Agreement required per submission.

AUTHOR:

Name:

Florian Ströhl

Department:

Department of Chemical Engineering and Biotechnology

Institution:

University of Cambridge, UK

Article Title:

A guide to fast multicolour TIRF-SIM

Signature:

F. Ströhl

Date:

31/07/2015

Please submit a signed and dated copy of this license by one of the following three methods:

- 1) Upload a scanned copy as a PDF to the JoVE submission site upon manuscript submission (preferred);
- 2) Fax the document to +1.866.381.2236; or
- 3) Mail the document to JoVE / Attn: JoVE Editorial / 17 Sellers St / Cambridge, MA 02139

For questions, please email editorial@jove.com or call +1.617.945.9051.

MS # (internal use):

Review comments rebuttal

We would like to thank all the reviewers for their time and appreciate their help in improving the manuscript. We have supplied additional representative results (figures and movies) showing applications of the technique for imaging live cells.

Editorial comments:

*1) All of your previous revisions have been incorporated into the most recent version of the manuscript. In addition, Editor may have made formatting changes and minor copy edits to your manuscript. On the JoVE submission site, you can find the updated manuscript under "file inventory" and download the microsoft word document. **Please use this updated version for any future revisions and track all changes using the track changes function in Microsoft Word.***

2) Prior to peer review, the highlighted portion of your protocol exceeds our 2.75 page highlighting limit. After making all the requested changes to the protocol, please adjust the highlighting to identify a total of 2.75 pages or less of protocol text (which includes sub-headings and spaces) that should be visualized to tell the most cohesive story of your protocol steps. The highlighting should include complete statements and not portions of sentences. See JoVE's instructions for authors for more clarification.

3) Formatting:

a) A space is required between steps 4.4.2 and 4.4.3.

A space has been added.

b) References – Please abbreviate all journal titles.

Reference style updated.

4) Grammar: Please use the American English spelling for all words in the manuscript.

Spelling has been changed to American English.

5) Visualization:

a) Section 1 – Please provide labeled photographs of the setup as a supplemental file. Please upload these files to the "Supplemental File (as requested by JoVE)" section of the JoVE submission site. Please add the suffix "_SW" for any files uploaded for this purpose.

Two labelled photographs of the setup have been included as supplementary files.

b) Please clarify "Separate the objective, lenses L3, L4, L5, and the SLM each by the sum of their respective focal lengths such that the SLM surface will be relayed onto the focal plane of the objective." It is unclear what action will be filmed here. This sentence does not require filming and we have removed the highlighting of corresponding text.

6) Additional detail is required:

a) 1.9 – How is the position adjusted?

Additional detail added.

b) 3.6 – How is the spatial mask inserted?

Additional detail added.

7) Please remove branded term from the 4.6 note: LabVIEW

Removed.

8) In Discussion, please include a discussion on the future applications of the technique.

A discussion of the future applications of the technique has been included at the end of the manuscript.

9) Please modify your references section to comply with JoVE's instructions for authors, specifically when there are more than 6 authors, list only the first author then "et al." Currently, two authors are listed, then et al.

Reference style has been updated.

10) Please take this opportunity to thoroughly proofread your manuscript to ensure that there are no spelling or grammatical errors. Your JoVE editor will not copy-edit your manuscript and any errors in your submitted revision may be present in the published version.

11) Please disregard the comment below if all of your figures are original.

If you are re-using figures from a previous publication, you must obtain explicit permission to re-use the figure from the previous publisher (this can be in the form of a letter from an editor or a link to the editorial policies that allows you to re-publish the figure). Please upload the text of the re-print permission (may be copied and pasted from an email/website) as a Word document to the Editorial Manager site in the "Supplemental files (as requested by JoVE)" section. Please also cite the figure appropriately in the figure legend, i.e. "This figure has been modified from [citation]."

Reviewers' comments:

Reviewer #1:

We would like to thank the reviewer for their helpful comments and address the points raised individually below.

Manuscript Summary:

The manuscript detailed the parts and steps required for successfully building a TIRF-SIM setup.

Major Concerns:

From the diagram alone (Fig 1), it's hard to understand the SIM pattern-generation

mechanism. What are the polarization states of the light incident on the SLM for the three orientations?

We have added arrows showing the linear polarization state of the illumination light incident on the SLM. The light should be azimuthally polarized to produce the maximum modulation contrast in the interference pattern and this is explained in the Introduction under “Polarization control”.

How is light modulated by the SLM such that it acts as a grating? These are crucial information because the mechanism here seems different from two major previous works (citations 13 and 16).

We have added an additional paragraph in the introduction to clarify the pattern generation mechanism. The binary phase SLM operates as a phase diffraction grating as each pixel imparts either 0 or π phase shift to the incident wave. Our implementation uses off axis illumination configuration (as previously used in citation 16, 18 and 28) compared to on axis as presented in citation 13. As citation 13 states, “Half of the power is lost in the final polarizing step” when using on axis illumination as the reflected beam from the SLM must traverse a polarizing beam splitter, but this is not the case for the off axis configuration as the polarization control is performed before the light is incident on the SLM. In citation 16, a QWP is used to produce circular polarization which is then passed via a fixed segmented polarizer to produce linear polarization for each of the 3 pattern angles. This method is passive and therefore removes the need for electro-optic control of polarization, but again half the power is lost due to the polarizer.

Minor Concerns:

-First paragraph: seems incomplete because it goes on about SMLM's pros and cons at length but then doesn't mention those for STED at all.

We have added an additional paragraph mentioning the advantages of STED over SIM and SMLM.

-Line 79--80: statement not true any more because since OMX Blade version, no rotation or translation of the grating is done.

This is of course correct and we have modified this statement.

-Line 200--203: "The arrangement shown in Figure 1" shows DM3 and DM4 both reflect around an axis that is normal to the paper. If that's the case, no such polarization compensation would occur. Use words to explain what 2D drawings cannot express.

This was unclear and we have added further explanation in the note to step 1.3. We have added also axis labels to the figure which will also help to clarify the arrangement.

-Step 1.4.2: Needs to emphasize that the pinholes have to be big enough to not clip the laser beam.

The original wording was unclear. We referred to alignment disks (Thorlabs) used to steer the beam incorrectly as pinholes; beam clipping is not an issue here. We have corrected this point to avoid confusion.

-Step 2.2: It's unclear what's being sought after here. Please provide more details including angular positions of the crossed polarizers, the retardance the LCVR is set to, etc. Also,

explain the role of the polarizer "P" in-between "M" and "HWP" in Fig 1. Isn't the laser beam already linearly polarized?

The LCVR can be physically mounted with its axis at 45° to the incident vertically polarized light, but this is only a rough alignment. The manufacturing tolerances of the device mean that the fast axis is actually slightly off when the device is mounted in the apparent “45°” position. The HWP is just used to slightly rotate the incident linear polarization and align it to exactly 45°.

The reviewer is correct to say that the laser diodes produce beams that are vertically linearly polarized, but we found that there is a very small amount of ellipticity introduced after reflection from the dichroic mirrors so we add an additional polarizer here to ensure perfectly linear polarization.

-Step 4.4.4: What's "the calibration process"? When is it "complete"? A lot more details are needed.

We have added an additional note in step 4.4.3 to clarify the purpose of this calibration procedure. The voltage applied to the LCVR is swept from minimum to maximum which has the effect of rotating the linear polarization incident on the sample. The modulation contrast is measured by calculating the ratio of the total signal in the first to the total signal in the zeroth-order Fourier components. We have included an additional MATLAB file (calculate_contrast.m) to demonstrate this.

Additional Comments to Authors:

N/A

Reviewer #2:

Manuscript Summary:

This manuscript describes implementation of a TIRF SIM microscope system using commercially available components, including construction and alignment of the optical system along with some simple testing procedures. For the most part the manuscript is appropriately detailed clearly written, however requires some additional detail on image reconstruction. In the opinion of this reviewer it is insufficient to simply reference existing literature covering SIM image reconstruction and, at the very least, the authors should include a high level overview of how their recommended reconstruction method. Once this point has been addressed, along with the minor concerns listed below the manuscript is suitable for publication in JoVE.

Major Concerns:

**The authors should provide a description of the image reconstruction methodology, including accurate determination of the illumination pattern parameters and recombination of SIM information passbands*

[Editorial recommendation: *The above comment may be addressed in the Introduction or Discussion.*]

We thank reviewer #2 for this comment and also the editors for allowing us to address this point and have added a few additional paragraphs in the introduction.

Minor Concerns:

**Lines 59 - 60: replace microscope with microscopy in '...stimulated emission depletion microscopy...' and '...structured illumination microscopy.'*

Fixed.

**Lines 81 - 83: I don't think it is correct that only custom-built SIM systems offer high temporal resolution - I think the later generations of the OMX SIM system offer single slice frame rates of several Hz*

As stated in the response to reviewer #1 to their similar comment, we have removed this statement.

**Line 97: why is SIM TIRF only possible with 2 of the 3 lasers?*

TIRF-SIM is only possible with 488 and 640 due to the constraints on the SLM pattern: the grating period must be chosen to fit the foci in the TIR ring while also being divisible by 3 to allow 3 equally spaced phase shifts. For 561, the period 9 or 12 patterns used don't fit within the TIR ring for this wavelength so TIRF-SIM isn't possible. Note that this is not a fundamental limitation of the technique.

**Line 174 - Choice of lenses: the stated critical angle presumably applies to a glass-water interface - this should be stated in the text. For samples of higher refractive index the critical angle will increase.*

Yes this is correct, we have clarified that this critical angle is for glass-water interfaces. For samples of higher refractive index, the critical angle increases and can result in scattering of the evanescent field, for example, at focal adhesions. This frustrated TIR seems to vary depending on the cell type, and we haven't seen it in the COS7 or HEK cell samples presented here.

**Lines 313 onward: many of the instructions obviously relate to specific devices and software packages, for example line 314 refers to specific tabs in the SLM control software. I'm not sure that this level of detail is required and arguably makes the instructions more difficult to follow.*

[Editorial recommendation: Please keep JoV'sE protocol requirements in mind as you address the above comment - the protocol must contain sufficient details in order to enable users to accurately replicate your technique. In addition these details are required for our scriptwriters to most accurately plan and write for your video. We recommend NOT removing any details from the protocol text.]

**Line 358: it would be helpful to include images showing how the image of the fluorescent solution changes between TIRF and non TIRF*

Yes this is important and useful to highlight so we have expanded Figure 2 to include images of TIRF and non-TIRF illumination that clearly show the misalignment effects.

**Spherical aberration (for example caused by variations in coverglass thickness) can be a significant problem in SIM microscopy. It would be useful if the authors discuss this - presumably the objective lens has a correction collar?*

We agree that spherical aberration is a huge problem for SIM and have added a sentence in the introduction suggesting use of a correction collar. For 3D-SIM it is extremely important to reduce spherical aberrations to maintain high pattern contrast at depth but for TIRF-SIM it seems to be less of an issue.

**The caption to Fig. 2 is slightly misleading. Reduced overlap between the beams decreases the field of view over which the sinusoidal excitation pattern is formed.*

Yes you are correct and we have modified the caption.

**Fig.5 - the image of carbocyanine labelled β -amyloid fibrils appears to suffer from artefacts (weak copies of filaments at either side of the main filament). These are not present in the image of the Rhodamine labelled fibrils. Could the authors comment on this.*

We have combined Figure 4 and 5 on the suggestion of Reviewer #3. The artefacts seen in the carbocyanine fibrils were ringing artefacts from the reconstruction due to the high dynamic range of the sample. The sidelobes result from the use of the Wiener filter reconstruction method and could have been reduced by empirically altering the Wiener parameter, or by using another reconstruction method which is less prone to this type of artefact.

Additional Comments to Authors:

N/A

Reviewer #3:

Manuscript Summary:

The protocol by Young et al. describes the built up of a custom design TIRF-SIM setup enabling super-resolution imaging with down to 90-120 nm lateral resolution of specimen/features that are accessible in the range of <200 nm from the coverslip surface.

The system outperforms commercial TIRF-SIM systems (Nikon N-SIM) in terms of acquisition speed through the replacement of a mechanical phase grating with a spatial light modulator. At the same time it should come with a considerably reduced price-tag (although the authors do not specifically mention this).

The manuscript provides a potentially useful instruction for laboratories that have in-house expertise to build custom optical setups and want to study a suitable biological question that benefits from the 2-fold lateral resolution enhancement over conventional TIRF setups. That said, the manuscript still needs some improvement to firmly justify publication in the JoVE.

These are valid comments and we have expanded the discussion both in the *future applications* and *potential modifications* sections of the manuscript. We have now included new data of dynamic biological processes (movies 1 and 2) that clearly demonstrate the

capability of the instrument and the advantages that come with TIRF SIM, offering both increased resolution and contrast.

Major Concerns:

**TIRF-SIM is geared toward particular samples and biological questions, typically addressing 2D cell surface biology that is within the reach of TIRF microscopy. The authors should mention this specialisation (or limitation) in applicability more thoroughly.*

On the other hand, if the system is not strictly restricted to operate in TIRF mode, the authors may consider describing or discussing options to use the instrument in other modes (e.g. far-field imaging, z-stack acquisition, or axial resolution increase by optional 3-beam interference).

We have made this limitation more clear in the discussion, and have included further details on how the system presented can be extended to other imaging modalities such as fast 2D-SIM, MSIM and PA NL-SIM.

**One major advantage of SIM versus SMLM is the ability to study live samples with higher frame rates and lower photodamage. Although the authors claim frame rates of up to 20 Hz for their system, they do not show any live cell data to support that this is not only a theoretical possibility.*

We have included several examples of high speed live cell TIRF-SIM in a new figure and have provided movies that clearly resolve high speed microtubule dynamics and plasma membrane flow and demonstrate the fast acquisition rate.

**The description or discussion of camera, microscope stage, sample holder, temperature control, software for acquisition, reconstruction, data quality control, DSP is rather rudimentary. By following the protocol in its current form it may be hard to replicate an operational setup. If not all aspects can be discussed in detail for space restrictions, it should be at least very explicitly stated which additional instructions or readings have to be followed.*

This protocol is *not* intended for a lay audience, it requires prior optics expertise. It is suited to a laboratory that is already engaged in optical microscopy development: many biophysics laboratories for example have home built TIRF microscopy set-ups. It should be a relatively straightforward matter for an experienced microscopist with optics expertise to follow the instructions. We have now added a paragraph to the protocols to say that Labview code we have written for our system is available on request.

Minor Concerns:

**(Line) 81 "Imaging with high temporal resolution is therefore only achievable with custom-built systems"*

This is not true for all commercial systems. GE's OMX Blaze 3D-SIM system uses arrays of galvo scanner to change angle and phase positions of the two first order beams

independently for each channel, which is in fact faster than any current SLM-based systems. GE's most recent OMX SR model also allows operation in 2D-SIM and 2D-SIM-TIRF mode. We have removed this statement and have instead emphasized the reduced cost and increased flexibility of this system compared to commercial instruments.

**535ff "Custom-built TIRF-SIM systems are capable of multicolour super-resolution imaging at high speed compared to commercially available microscopes. (see above) The inherent advantage of SIM as a super-resolution technique is that the temporal resolution is not limited by the photophysics of the fluorophore... "*

One could argue that this also applies to SIM, as photophysical properties such as bleaching rate or quantum efficiency affect the minimum exposure time and the number of time points that can be recorded with sufficient signal-to-noise.

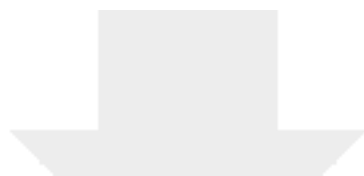
The reviewer is correct and we have discussed this under “limitations of the technique”.

**541ff "Non TIRF-SIM systems can usually achieve resolution improvements of 1.7 times or less in practice as opposed to the factor of 2 improvement reported here, and commercial systems are also slower and less flexible than the system presented in this protocol."*

That is surely an overstatement. While this may be true for many instruments in the field (and maybe based on the personal experience of the authors), a well-calibrated and well-operated 3D-SIM system used on sufficiently contrasted samples can routinely achieve 2-fold resolution improvement, as has been demonstrated in many publications (see e.g. Demmerle et al. 2015, Methods 88).

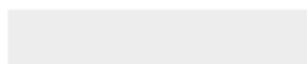
We have modified the sentence to reflect the reviewer's concerns.

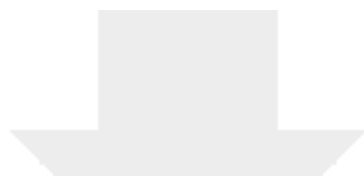
All other minor comments/edits have been addressed in the manuscript with appropriate changes to text and figure captions.



[Click here to access/download](#)

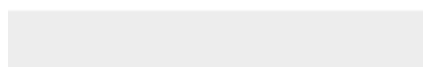
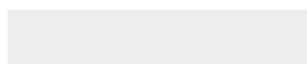
Supplemental File (as requested by JoVE)
setup_figure1_SW.png





[Click here to access/download](#)

Supplemental File (as requested by JoVE)
setup_figure2_SW.png

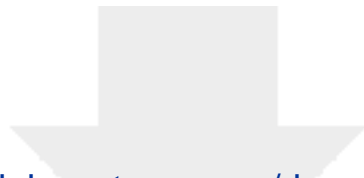




[Click here to access/download](#)

Supplemental code file (if applicable)
48449 300us 1-bit Balanced.seq3

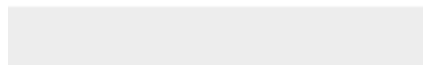


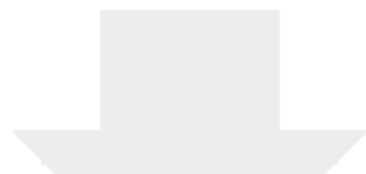


[Click here to access/download](#)

Supplemental code file (if applicable)

period9_001.bmp

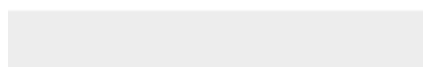
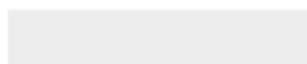


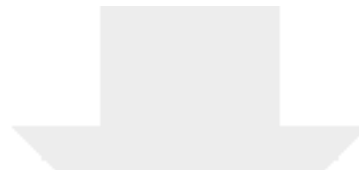


[Click here to access/download](#)

Supplemental code file (if applicable)

period9_002.bmp

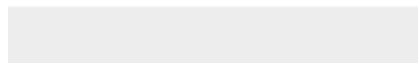
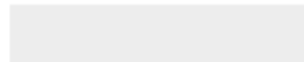


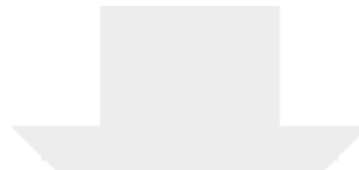


[Click here to access/download](#)

Supplemental code file (if applicable)

period9_003.bmp

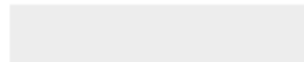


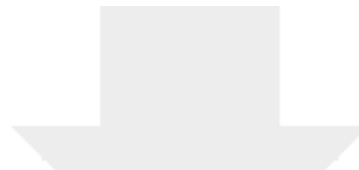


[Click here to access/download](#)

Supplemental code file (if applicable)

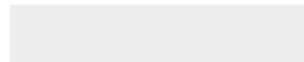
period9_004.bmp

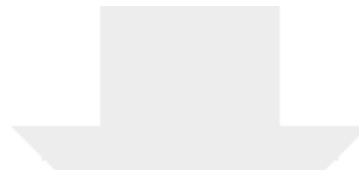




[Click here to access/download](#)

Supplemental code file (if applicable)
period9_005.bmp

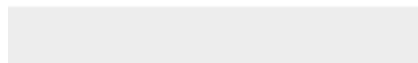


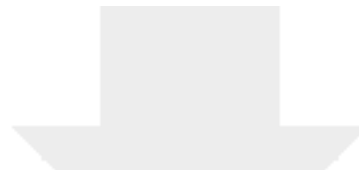


[Click here to access/download](#)

Supplemental code file (if applicable)

period9_006.bmp

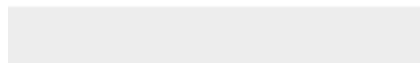
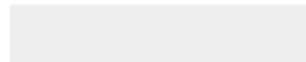


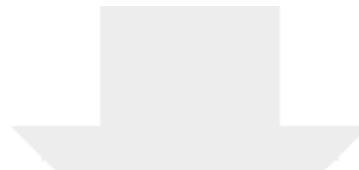


[Click here to access/download](#)

Supplemental code file (if applicable)

period9_007.bmp

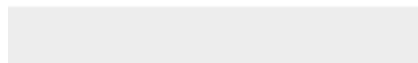


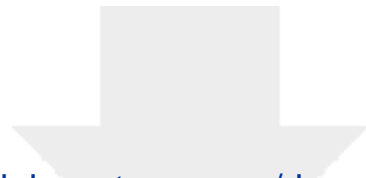


[Click here to access/download](#)

Supplemental code file (if applicable)

period9_008.bmp

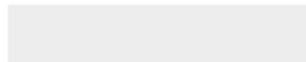




[Click here to access/download](#)

Supplemental code file (if applicable)

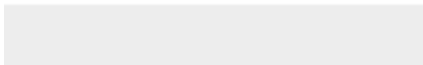
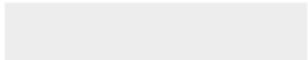
period9_009.bmp





[Click here to access/download](#)

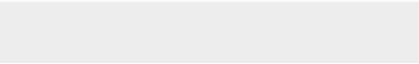

Supplemental code file (if applicable)
[period9_mask_1.bmp](#)





[Click here to access/download](#)

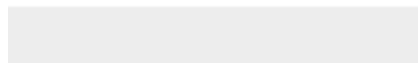
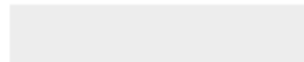
Supplemental code file (if applicable)
[period9_mask_2.bmp](#)





[Click here to access/download](#)

Supplemental code file (if applicable)
period9_mask_3.bmp





[Click here to access/download](#)

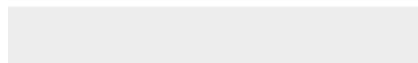
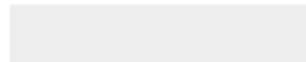
Supplemental code file (if applicable)

TIRF-SIM_example.rep



[Click here to access/download](#)

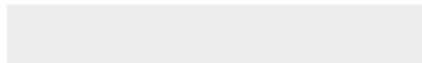
Supplemental code file (if applicable)
`generate_gratings.m`

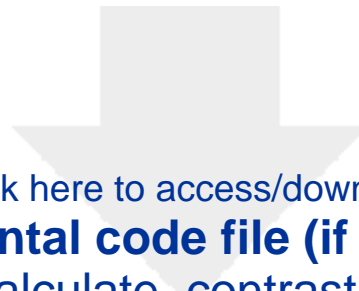




[Click here to access/download](#)

Supplemental code file (if applicable)
`circular_mask.m`





[Click here to access/download](#)

Supplemental code file (if applicable)
`calculate_contrast.m`

